Comparison of Control Strategies for Dividing-Wall Columns

ARTICLE *in* INDUSTRIAL & ENGINEERING CHEMISTRY RESEARCH · JANUARY 2010

Impact Factor: 2.59 · DOI: 10.1021/ie9010673

Comparison of Control Strategies for Dividing-Wall Columns

Ruben C. van Diggelen,[†,‡] Anton A. Kiss,[*,†] and Arnold W. Heemink[‡]

AkzoNobel—Research, Development & Innovation, Process & Product Technology, Velperweg 76, 6824 BM, Arnhem, The Netherlands, and Institute of Applied Mathematics, Delft University of Technology, Mekelweg 4, 2628 CD Delft, The Netherlands

Conventional ternary separations progressed via thermally coupled columns such as Petlyuk configuration to a novel design that integrates two distillation columns into one shell—a setup known today as dividing-wall column (DWC). The DWC concept is a major breakthrough in distillation technology, as it brings significant reduction in the capital invested as well as savings in the operating costs. However, the integration of two columns into one shell leads also to changes in the operating mode and ultimately in the controllability of the system. Although much of the literature focuses on the control of binary distillation columns, there are just a few studies on the controllability of DWC. In this work we explore the DWC control issues and make a comparison of various control strategies based on PID loops, within a multiloop framework (DB/LSV, DV/LSB, LB/DSV, LV/DSB) versus more advanced controllers such as LQG/LQR, GMC, and high order controllers obtained by H_∞ controller synthesis and μ-synthesis. The controllers are applied to a dividing-wall column used in an industrial case study—the ternary separation of benzene−toluene−xylene. The performances of these control strategies and the dynamic response of the DWC is investigated in terms of product composition and flow rates, for various persistent disturbances in the feed flow rate and composition. Significantly shorter settling times can be achieved using the advanced controllers based on LQG/LQR, H_∞ controller synthesis, and μ-synthesis.

1. Introduction

As a thermal separation method, distillation is one of the most important separation technologies in the chemical industry. Basically, all of the chemicals produced worldwide go through at least one distillation column on their way from crude oil to final product. Considering its many well-known benefits, distillation is and will remain the separation method of choice in the chemical industry—with over 40 000 columns in operation around the world. Despite the flexibility and the widespread use, one important drawback is the considerable energy requirements, as distillation can generate more than 50% of plant operating costs.[1] An innovative solution to reduce this drawback is using advanced process integration techniques.[2]

Conventionally, a ternary mixture can be separated via a direct sequence (most volatile component is separated first), indirect sequence (heaviest component is separated first), or distributed sequence (midsplit) consisting of two to three distillation columns. This separation sequence evolved to the Petlyuk column configuration[3] consisting of two fully thermally coupled distillation columns. Eventually, this led to the concept known today as dividing-wall column (DWC) that integrates in fact the two columns of a Petlyuk system into one column shell.[4−7] Figure 1 illustrates the most important ternary separation alternatives.

The name of DWC (dividing-wall column or divided wall-column) is given because the middle part of the column is split into two sections by a wall, as illustrated in Figure 1. Feed, typically containing three or more components, is introduced into one side of the column facing the wall. Deflected by the wall, the lightest component A flows upward and exits the column as top distillate while the heaviest component C drops down and is withdrawn from the bottom of the column. The intermediate boiling component B is initially entrained up and down with both streams, but the fluid that goes upward subsequently separates in the upper part and falls down on the opposite side of the wall. Similarly, the amount of B that goes toward the bottom separates in the lower part and then flows up to the back side of the wall, where the entire B product is recovered by a side draw stream. Note however that using a DWC requires a proper match between the operating conditions of the two stand-alone columns in a conventional direct or indirect sequence.[8]

DWC is very appealing to the chemical industry—with Montz and BASF as the leading companies[9]—because it can separate three or more components in a single tower, thereby eliminating the need for a second unit, hence saving the cost of building two columns and cutting operating costs by using a single condenser and reboiler. In fact, using dividing-wall columns can save up to 30% in the capital invested and up to 40% in the energy costs,[6,10,11] particularly for close boiling species.[12] In addition, the maintenance costs are also lower.

Compared to classic distillation design arrangements, DWC offers the following benefits:

- high purity for all three or more product streams reached in only one column
- high thermodynamic efficiency due to reduced remixing effects
- lower capital investment due to the integrated design
- lower energy requirements compared to conventional separation sequences
- small footprint due to the reduced number of equipment units

Moreover, the list of advantages can be extended when DWC is further combined with reactive distillation leading to the more integrated concept of reactive DWC.[11,13] Note however that the integration of two columns into one shell leads also to changes in the operating mode and ultimately in the controllability of

* To whom correspondence should be addressed. Tel.: +31 (0)26 366 1714. Fax: +31 (0)26 366 5871. E-mail: Tony.Kiss@akzonobel.com.
† AkzoNobel.
‡ Delft University of Technology.

10.1021/ie9010673 CCC: $40.75
Published on Web 11/09/2009

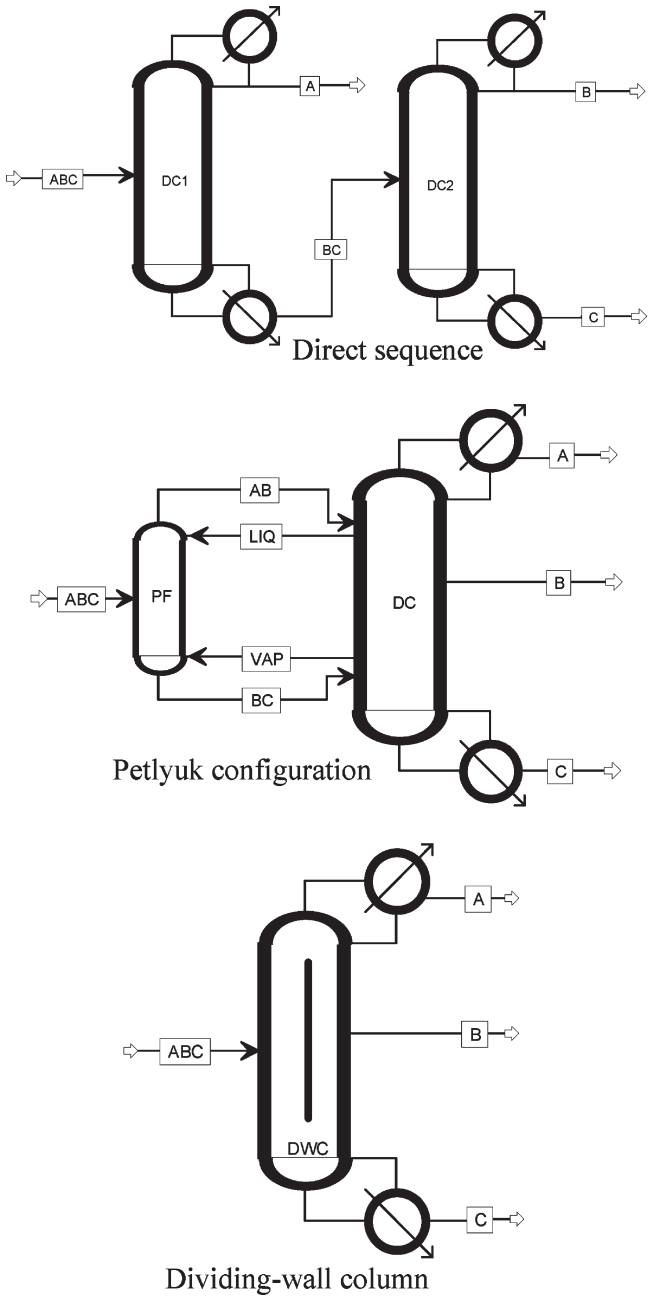

Figure 1. Separation of a ternary mixture via direct distillation sequence (top), Petlyuk configuration (center), and dividing-wall column (bottom).

the system.[14] Therefore, all these benefits are possible only under the condition that a good control strategy is available and able to attain the separation objectives.

Although much of the literature focuses on the control of binary distillation columns, there are only a limited number of studies on the control of DWC. The brief literature review that follows makes a critical overview of the most important DWC control studies up to date.

In this work we explore the main DWC control issues and make a comparison of various control strategies based on proportional integral derivative (PID) loops within a multiloop framework (DB/LSV, DV/LSB, LB/DSV, LV/DSB), more advanced controllers such as LQG/LQR, GMC, and high order controllers obtained by H_∞ controller synthesis and μ-synthesis. The performance of these control strategies and the dynamic response of the DWC is investigated in terms of product composition and flow rates, for various persistent disturbances

Table 1. Physical Properties of the Investigated Ternary System: Benzene, Toluene, and Xylene

physical property	benzene	toluene	xylene
molecular formula	C_6H_6	C_7H_8	C_8H_{10}
molecular weight	78.11	92.14	106.17
density (kg/m^3)	878.6	866.9	860.0
viscosity (cP at 20 °C)	0.652	0.590	0.620
critical pressure (bar)	48.95	41.08	35.11
critical temperature (°C)	288.9	318.6	343.05
melting temperature (°C)	5.53	−94.97	13.26
boiling temperature (°C)	80.09	110.63	138.36

in the feed flow rate and composition. These control strategies are applied to an industrial case study—a dividing-wall column used for the ternary separation of benzene−toluene−xylene (physical properties listed in Table 1).

2. Literature Review

The literature study reveals that a variety of controllers are used for distillation columns. Although there is an abundance of literature available about distillation control, most of the studies are on the control of binary separations. Some of them are mainly interesting from a theoretical point of view, while others present a more practical approach.

Viel et al.[15] proposed a stable control structure for binary distillation column based on a nonlinear Lyapunov controller. The controller satisfied the design goals to maintain the product qualities at their given set points, despite the presence of typical disturbances in the feed flow rates and in the feed composition. The model used to design the controller is a relatively simple constant molar overflow model. In such a model pressure is taken to be constant, and thermal balances are neglected. The performance of the controller was compared with another nonlinear controller[16] based on the input−output linearization (IOL) technique.[17] Therefore, this Lyapunov based controller can achieve set point tracking and asymptotic disturbance rejection with better robustness than in the case of using a decoupling matrix obtained by input−output linearization.

In addition to nonlinear control structures, Biswas et al.[18] augmented IOL controllers with quadratic matrix controller (IOL-QDMC). The performance of this controller was compared to a quadratic dynamic matrix controller and input−output linearization with PI controller (IOL-PI). Consequently, the two nonlinear controllers performed better than the linear model predictive controller (QDMC). In the presence of unmeasured disturbance to the process and parametric uncertainty, the IOL-QDMC is much better than simple IOL-PI.

The generic model control (GMC) described by Lee and Sullivan[19] is a process model based control algorithm that incorporates the nonlinear model of the process directly within the control algorithm. In addition to this, a variant of GMC also known as distillation adaptive GMC (DAGMC) was applied to two typical nontrivial distillation units.[20] Note that when the relative order of a nonlinear system is equal to 1, the control law of GMC is the same as the control law obtained by IOL.[21]

A different robust controller was designed by Gu.[22] The control structure consisted of a two-level control: inventory control and composition control. The inventory of the nonlinear model was simply done by two P controllers. Here, the inventory control is done by the level control of the tank liquid level (H_T) and the level control of the reboiler (H_R). The composition control is done by a two-degrees-of freedom (2DOF) H_∞ controller obtained by a loop shaping design procedure (LSDP) and a μ-controller obtained by μ-synthesis. The μ-controller ensures robust stability of the closed loop system and fulfillment

of a mixture of time domain and frequency domain specifications. Although the design of the controller is based on a reduced linearized model, the simulation of the closed loop system with the nonlinear distillation model shows very good performance for different reference signals (set point tracking) and disturbance signals (measurement noise and time delay).

Several authors studied the design phase of the dividing-wall column in order to improve the energy efficiency. The design stage of a DWC is very important as in this phase there are two DOF that can be used for optimization purposes. In this perspective we mention the study reported by Halvorsen and Skogestad[23] about understanding the steady-state behavior. The optimal solution surface of the minimal boil up is given as a function of the control variable *liquid split* (R_L) and the design variable *vapor split* (R_V)—defined in the Appendix. Furthermore, candidate outputs are suggested that can be used to control the system such that the boil up is minimized. One of the outputs is the measure of symmetry (DTs) in the temperature profile along the column. The measure of symmetry DTs is defined by Skogestad as $DT_s = \sum(T_{1,j} - T_{4,j}) + \sum(T_{2,j} - T_{5,j})$, where $T_{i,}j$ denotes the temperature from section i at tray j. In the case of optimal operation the temperature profile in the column is symmetric. Hence a 4×4 system is obtained where the inputs are reflux flow rate, vapor flow rate, side product flow rate, and liquid split (L_0, V_0, S, R_L), and the measured outputs are the three product purities and DTs (x_A, x_B, x_C, DTs), respectively. A suitable set point for the variable DTs makes sure that the operating point is on the bottom of the optimal solution surface—hence the boil up related to vapor flow rate is minimized.

A more practical approach is suggested by Serra et al.[24] A linearized model is used to obtain a feedback control by PI control. The inventory level consists of two PI loops in order to keep the liquid in the tank and the liquid in the reboiler at a nominal level. From the candidate manipulated variables of L_0, V_0, D, B, S, R_L, and R_V, typically DB, LB, DV, or LV is used for inventory control. The remaining variables can be used for composition control. Ideally, the controllability property of the column should be taken into account at the design stage. Serra et al.[25] compared two designs using linear analysis tools—Morari resiliency index (MRI), condition number (CN), relative gain array (RGA), and closed loop disturbance gain (CLDG)—although nonlinear analysis could also be applied.[26−28]

A more advanced approach for a DWC is the model predictive control (MPC) strategy reported by Adrian et al.[29] The MPC controller outperforms a single PI loop. Three temperatures are controlled by the reflux ratios, the liquid split, and the side-draw flow rate, respectively. The disturbed variable in this case was the feed flow rate.

The null space method is a self-optimizing control method that selects the control variables as combinations of measurements.[30] For the case of a Petlyuk distillation setup this resulted in the following candidate measurements: temperature at all stages and all flow rates. Using the null space method a subset of six measurements was obtained, resulting in a practical implementation.

The energy efficiency of the DWC may be improved by allowing heat transfer through the wall.[31] Although the energy savings that are obtained are small, their suggestion can be taken into account when one is designing a DWC unit.

Il Kim et al.[32] recommended general guidelines and rules for the design of the DWC and standards for selecting control structures for the DWC. These were used later in a few studies.

A very recent control structure is proposed by Ling and Luyben.[33] Their case study resulted in an energy minimizing control structure consisting of PID controllers. They concluded that the composition of the heavy component at the top of the prefractionator is an implicit and practical way to minimize energy consumption in the presence of feed disturbances. This specific composition was controlled by the liquid split variable (R_L).

Cho et al.[34] proposed a profile position control scheme for the control of a DWC with vapor side draw. Relative gain array (RGA) and singular value decomposition (SVD) analysis were used to determine the optimal control configuration. Dynamic simulation showed that the profile position−product composition cascade control can keep the product purities at the desired values in the face of feed and internal disturbances.

Controller performance can be benchmarked in a systematic way based on operating records (i.e., data from plant) or using a plant model.[35] For example, if a PID controller is required to control a plant, the LQG cost functions can be used to provide the lowest practically achievable performance bound. The optimal LQG based controller can be used then to compute the optimal PID controller. This optimal controller can be compared to the actual controller and hence the performance can be determined. This approach has been applied to a simulation of a DWC proprietary BASF.[35]

3. Problem Statement

Following the literature review, it is clear that while a variety of controllers are used for binary distillation columns, only a few control structures were studied for dividing-wall columns. In most of the cases PID loops within a multiloop framework controllers were used to steer the system to the desired steady state. However, control of a DWC using model predictive control has also been successfully studied.[29]

Nevertheless, there is still a gap between PID loops within a multiloop framework control structures and an MPC strategy. Hence, the applicability and possible advantage of more advanced control strategies should be investigated. Moreover, a major problem of the previously reported case studies is the difficulty if not imposibility of making a fair comparison of the control structures, as different ternary systems were used for separation in a DWC. To solve this problem, we apply all the investigated control structures to the same DWC, thus allowing a nonbiased comparison of the control performace.

The general design goal is to maintain the product qualities at their given set points even in the presence of the disturbances. In this work, the set points are chosen equally for the three product compositions. Moreover, since we try to achieve a sharp separation, there are no changes made to the set point. As a consequence, reference tracking—the performance of the overall system in case the reference changes—is not investigated. We exert two types of disturbances: 10% increase of feed flow rate and 10% increase of the molar fraction of the lightest component in the feed. Note also that the disturbances are not exerted simultaneously.

The time needed by the controller for steering the product purities in a small neighborhood of the set points after the exertion of disturbance is measured and used for comparison of the controller performance. Since in an industrial environment the measurements can be distorted by noise and measurement delays, we carry out additional simulations using the controllers that satisfy the general design goal. Hence, the controller performance is investigated in case of a measurement delay of 1 min and added measurement noise. The noise is filtered, which

results in a more peak-shaped noise signal instead of a block signal. The gain of the filter is such that the average noise strength is 1% of the nominal measured value.

4. Dynamic Model of DWC

The dynamic model proposed in this work is used to develop a controller; hence it is recommended to use linearized liquid dynamics instead of neglecting the liquid dynamics.[36] In the long run there is no difference between neglecting liquid dynamics and linearizing liquid dynamics. However, when the liquid dynamics are not neglected but simplified by a linearization, the initial response is more realistic. Hence, linearized liquid dynamics is incorporated in the model. Note that the vapor split is impractical to control hence it considered as a design variable—although with a variable vapor split the energy loss in the presence of feed disturbances is about 10 times lower than with a fixed vapor split.[30]

For the dynamic model a number of reasonable simplifying assumptions were made: (1) constant pressure, (2) no vapor flow dynamics, (3) linearized liquid dynamics, and (4) neglecting the energy balances and changes in enthalpy. Note that DWC is thermodynamically equivalent to the Petlyuk system that is modeled using the following equations:

$$\dot{\mathbf{x}} = f(\mathbf{x}, \mathbf{u}, \mathbf{d}, t)$$
$$\mathbf{y} = g(\mathbf{x}) \tag{1}$$

where $\mathbf{u} = [L_0\ S\ V_0\ D\ B\ R_L\ R_V]$ is the input vector, $\mathbf{d} = [F\ z_1\ z_2\ q]$ is the disturbance vector, $\mathbf{x}$ is the state vector consisting of compositions and liquid holdups, and $\mathbf{y} = [x_A\ x_B\ x_C\ H_T\ H_R]$ is the output vector.

The dynamic model is implemented in Mathworks Matlab,[37] and it is based on the Petlyuk model previously reported in the literature by Halvorsen and Skogestad.[23] For the detailed mathematical description of the model the reader is referred to the Appendix.

Figure 2 illustrates the simulated dividing-wall column. The column is divided into six sections, each containing eight trays, with a total of 32 trays in the main column and 16 in the prefractionator side. When disturbances are not present, the feed flow rate is assumed to be $F = 1$, the feed condition is $q = 1$ (saturated liquid), and there are equimolar compositions of A, B and C in the feed. The liquid holdups are set as follows: for the reflux tank and the reboiler the holdup is 20, for the prefractionator the liquid holdup is 0.5, and for the main column (sections 3, 4, 5, 6) the liquid holdup is 1, 0.5, 0.5, and 1, respectively. Furthermore, according to the assumptions the vapor flow is constant inside a section:

$$V_i = V_{i-1} \tag{2}$$

In addition, the linearized approximation for the liquid flow is given by

$$L_i \approx k_0 + k_1 H_i + k_2 V_{i-1} \tag{3}$$

where the constants k_0, k_1, and k_2 have to be chosen properly. Especially the constant k_2 has an impact on the control properties of DWC, while V is assumed to be a control variable.

Note that in the literature quite a range of set points for the product purities has been used for ternary separation. Most recent industrial examples mentioned are the separation of ternary mixtures: benzene−toluene−*o*-xylene[33] and benzene−toluene−*p*-xylene.[31] The authors used for the set points of the product purities the values [0.99 0.99 0.99] and [0.95 0.95 0.95],

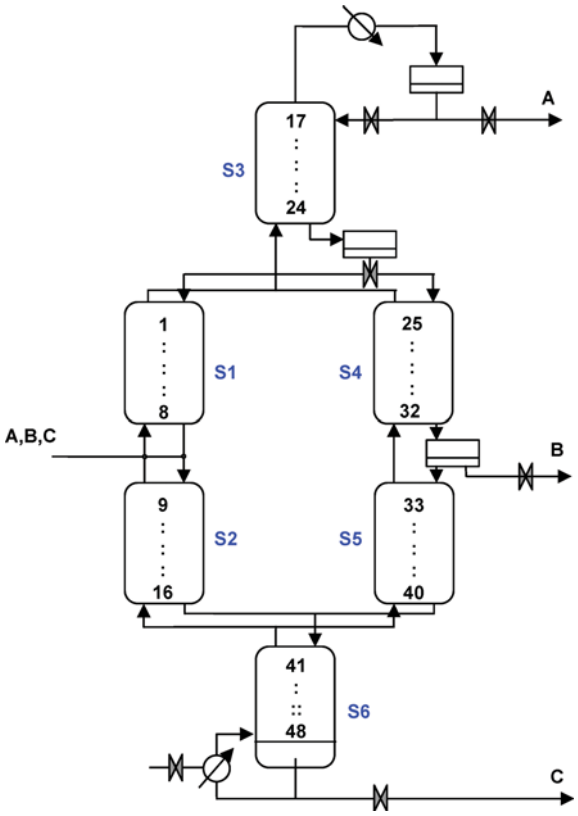

Figure 2. Schematics of the simulated dividing-wall column.

respectively. In this work, we use the same ternary mixture (benzene−toluene−xylene, equivalent to A, B, C) and the reasonable set points [0.97 0.97 0.97] for the product specifications. Figure 3 provides the composition profiles inside the simulated DWC by means of a ternary diagram, at various feed conditions ($q = 1$, saturated liquid; $q = 0$, saturated vapor; and $0 < q < 1$, mix of liquid and vapor). The bottom, side, and top products are close to the left, top, and right corners, respectively.

Linear Model. A local linear model around the steady state ($\mathbf{x}^*$,$\mathbf{u}^*$) is obtained by numerical differentiation using the formula

$$\frac{\partial f(\mathbf{x})}{\partial \mathbf{x}} = \frac{f(\mathbf{x} + h) - f(\mathbf{x} - h)}{2h} \tag{4}$$

Hence a state space model is obtained by computing the derivative of the functions f and g with respect to alternating $\mathbf{x}$ or $\mathbf{u}$. The model has 156 states (96 compositions for A and B; eight compositions for A and B in the two splitters, reflux tank, and reboiler; 48 tray holdups plus four additional holdups for the two splitters, reflux tank, and reboiler) and 11 inputs (five control, two design, and four disturbance variables), just as the nonlinear model. The quality of the linear model is clearly illustrated in Figure 4, where the nonlinear response and the linear response are given on a temporary disturbance in the feed flow rate. Note that the inputs were set at nominal level and only the tank and reboiler level were controlled while they appear to be unstable.

5. Control Strategies

PID Loops within a Multiloop Framework. The most used controllers in industry are the PID controllers.[38] In case of a DWC, two multiloops are needed to stabilize the column and another three loops are needed to maintain the set points

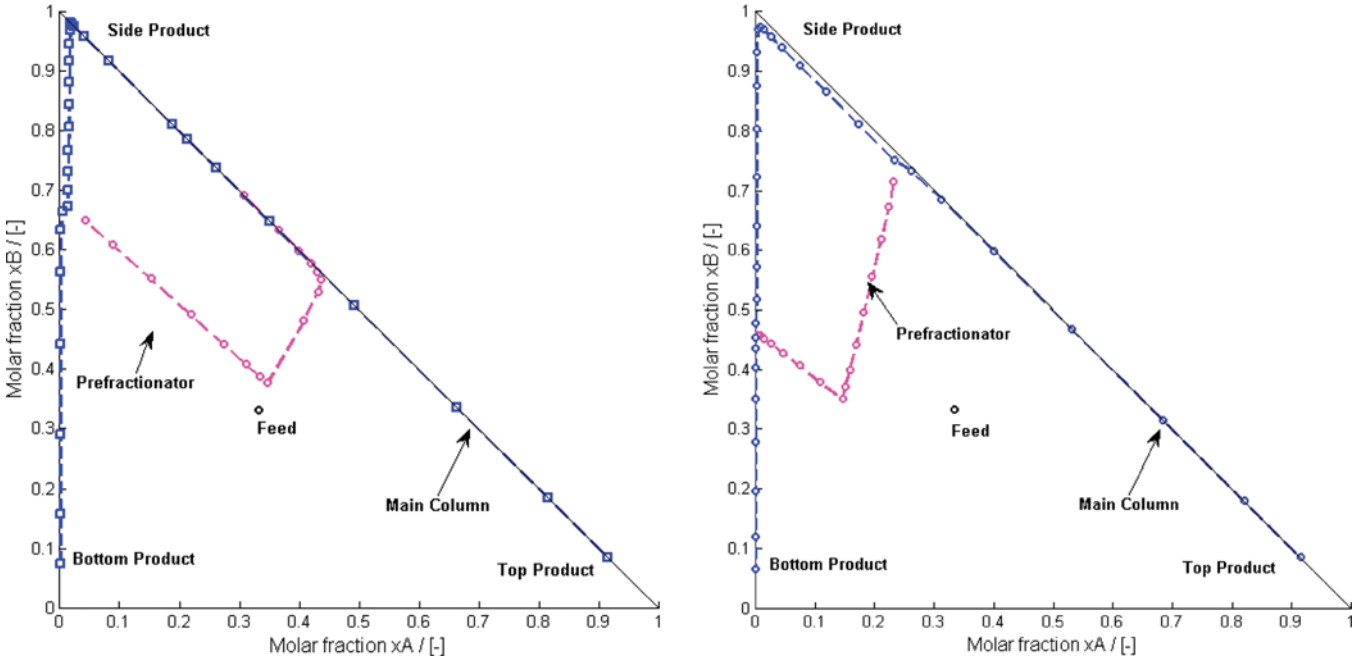

Figure 3. Composition profile inside the dividing-wall column, as ternary diagram for two cases: saturated liquid feed ($q = 1$, left) and liquid−vapor feed ($q = 0.5$, right).

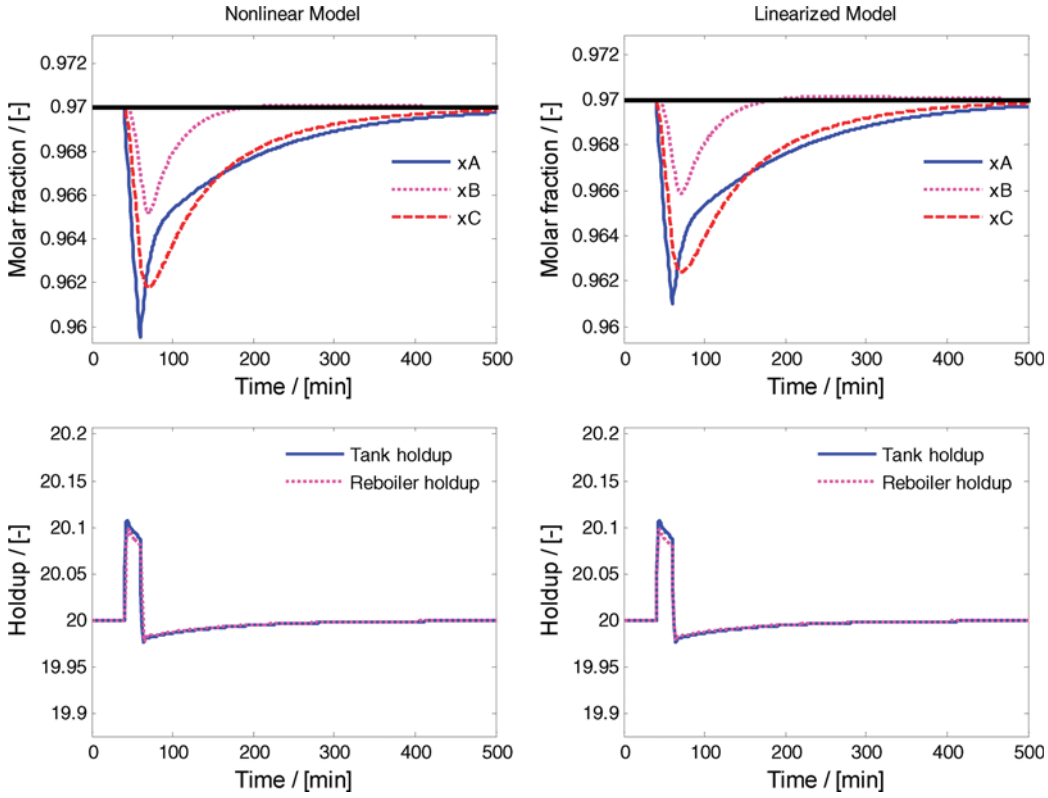

Figure 4. Comparison between the nonlinear and linearized systems: response after a nonpersistent disturbance of +10% in the feed flow rate for 20 min ($t = 40-60$).

specifying the product purities. While there are six actuators ($D\ S\ B\ L_0\ V_0\ R_L$) using PID loops within a multiloop framework, many combinations are possible. However, there are only a few configurations that make sense from a practical viewpoint. The level of the reflux tank and the reboiler can be controlled by the variables L_0, D, V_0, and B, respectively. Hence, there are four so-called *inventory control* options to stabilize the column, the combinations D/B, L/V, L/B, and V/D to control the level in the reflux tank and the level in the reboiler (Figure 5). The part for the control of product purities is often called *regulatory control*. One actuator is left (R_L) that can be used for optimization purposes such as minimizing the energy requirements.[23,33]

Moreover, closed loop stability of the decentralized PID control structure is an unsolved problem.[38] PID loops within a multiloop framework imply a tuning problem with many solutions and hence difficult to solve. Nevertheless, the PID loops within a multiloop framework are more or less model independent. Hence, if the true plant is quite different from the

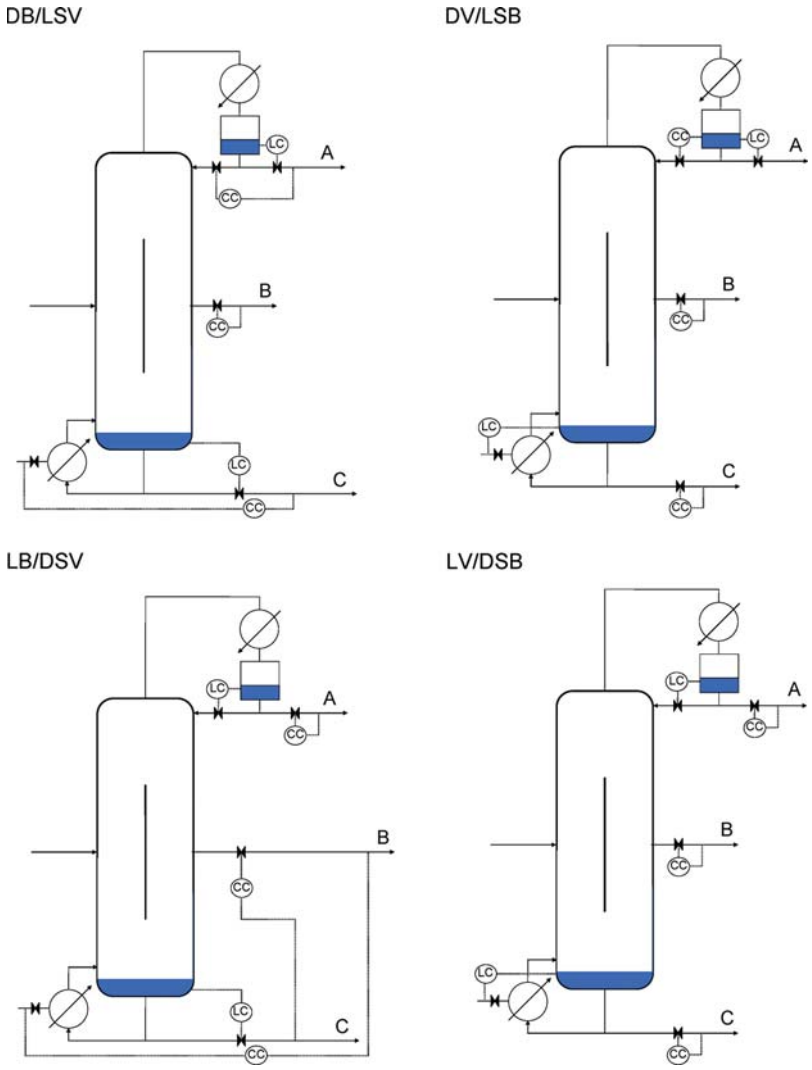

Figure 5. Control structures based on PID loops within a multiloop framework: DB/LSV, DV/LSB, LB/DSV, and LV/DSB.

model, it is likely that the control system will still work. Note that PI controllers in a multiloop framework control the system via a matrix structure with only one PI controller on each column. The full-order multiinput−multioutput (MIMO) problem has been successfully solved and it has in addition a useful cost criterion: linear quadratic Gaussian control.

Linear Quadratic Gaussian Control (LQG). LGC is a combination of an optimal controller LQR and an optimal state estimator (Kalman filter) based on a linear state space model with measurement and process noise which minimizes the cost function:

$$J_{\mathrm{LQ}} = \int_0^\infty \mathbf{x}(t)^{\mathrm{T}}\,\mathbf{Q}\mathbf{x}(t) + \mathbf{u}(t)^{\mathrm{T}}\,\mathbf{R}\mathbf{u}(t)\,\mathrm{d}t \qquad (5)$$

LQG is an extension of optimal state feedback that is a solution of the *linear quadratic regulation* (LQR) that assumes no process noise and assumes that the full state is available for control. Since in case of a DWC the full state is a priori not available, and measurement noise and disturbances are assumed in the feed, the state should be estimated taking into account the disturbances. While the LQG control deals only with zero-mean stochastic noise, it is not suitable for dealing with persistent disturbances in the feed.

The resulting offset can be solved using an additional feed-forward controller structure given in Figure 6. For example, if

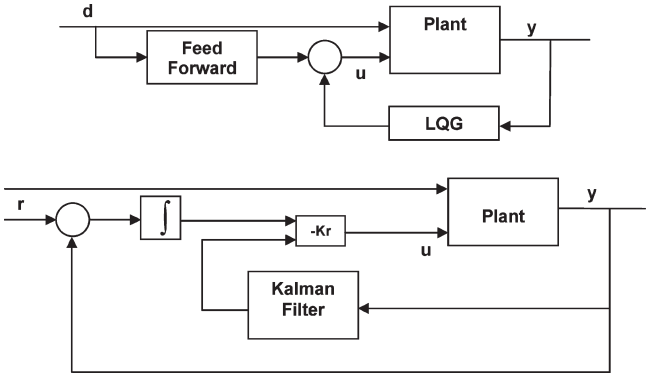

Figure 6. LQG controller with feed-forward controller (top); LQG controller extended with integral action (bottom).

the feed flow rate increases persistently by 10% the product flow rates also increase by 10% in order to reach a steady state. By measuring the feed flow rate, the changes can be used directly to adapt the product flow rates with the same percentage. However, for persistent disturbances in feed composition and condition, it is more difficult to tune the feed-forward controller. A working solution is to extend the LQG controller with an integral action.[39] The resulting controller structure is also shown in Figure 6. With an LQR controller there is no tuning problem, while the optimal feedback controller is given via an algebraic

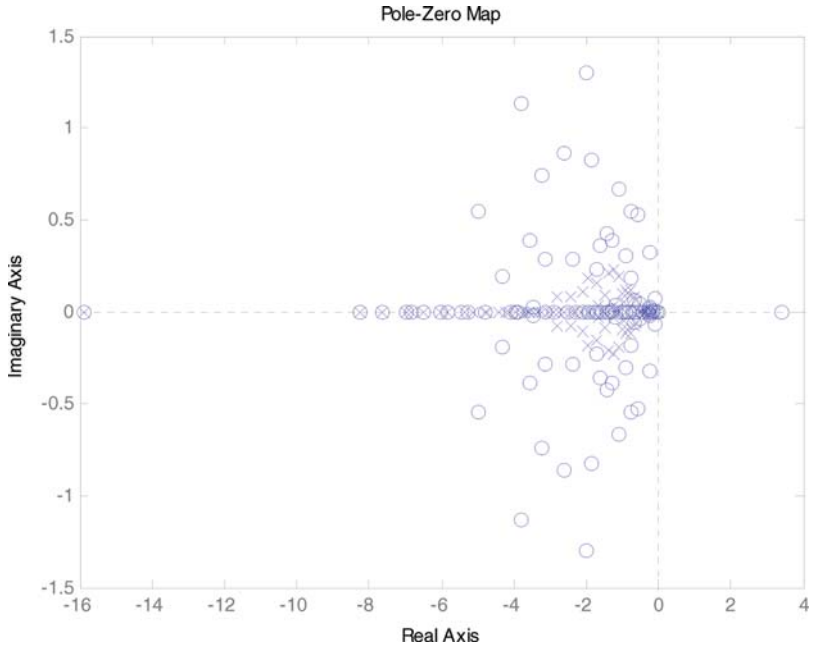

Figure 7. Pole−zero map of the linearized system.

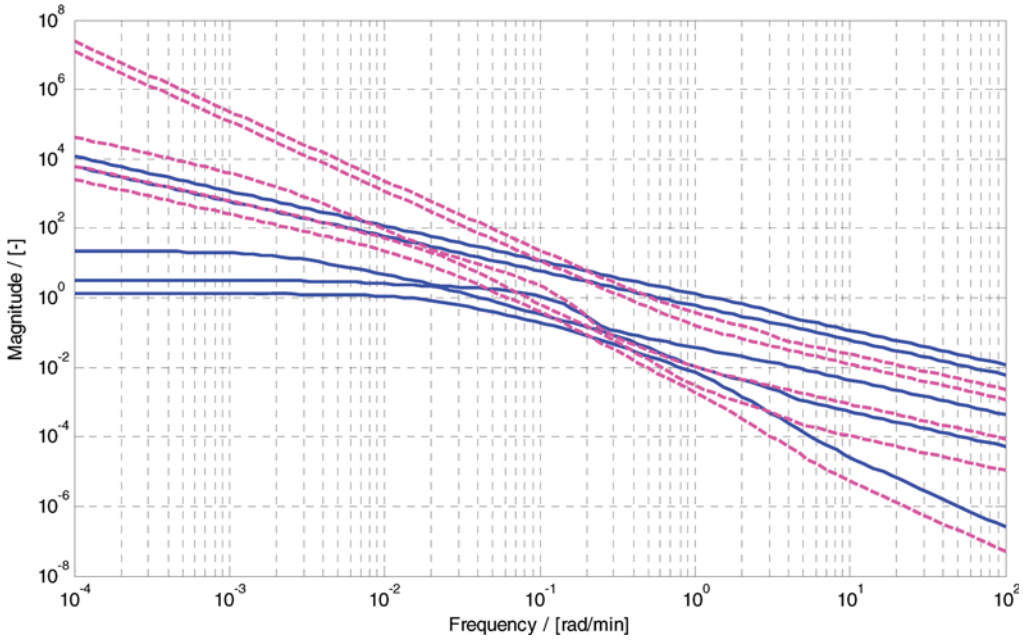

Figure 8. Frequency response of the plant G (—) and of the shaped plant G_s (---).

Ricatti equation (ARE). In addition, the closed loop system is stable with respect to zero-mean white noise. However, the obtained control structure depends heavily on the used linear model. Hence, a realistic linearized model is needed: with multivariate controller synthesis robust stability and robust performance can be obtained with respect to model uncertainty, and with nonlinear control the linearization step can be avoided.

Nonlinear Control. For distillation columns the nonlinear control was previously explored by Rouchon.[16] Basically the PID based controllers and LQG are linear controllers that need a linearization step in order to control a nonlinear system. Most likely this leads to a loss in the control action while the plant behaves nonlinear. For the control of binary distillation, nonlinear control has been successfully performed. For example, it is possible to control a binary distillation column using an input-output linearizing (IOL) controller.[18] However the controller is based on a reduced model only considering the bottom purity in the reboiler and the top purity in the reflux drum.

Generic Model Control (GMC). GMC is a process model-based control algorithm using the nonlinear state-space model of the process, and it is a special case of IOL if the system has a relative order of 1.[40] This can be done directly by solving the nonlinear equation for the input **u**:

$$\frac{\partial \dot{g}}{\partial \mathbf{x}^{\mathrm{T}}} f(\mathbf{x}, \mathbf{u}, \mathbf{d}, t) = K_1(\mathbf{y}^* - \mathbf{y}) + K_2 \int_0^t (\mathbf{y}^* - \mathbf{y})\, \mathrm{d}t \quad (6)$$

The interpretation is that the derivative of the output **y** with respect to time follows the predefined PI-control signal at the right-hand side. The full state is needed and in case the plant is approximated by a linear model the left-hand side can be replaced with the linear equivalent, where $\mathbf{y}^*$ is a vector of set

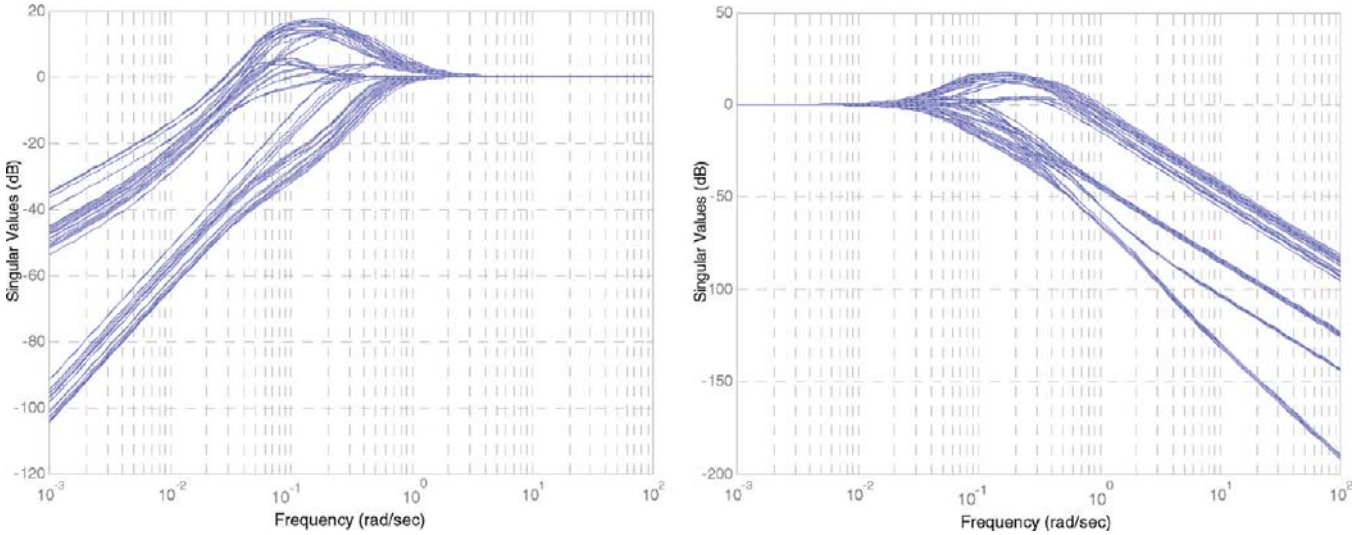

Figure 9. Singular value plots of the sensitivity function S (left) and the complementary sensitivity function $T = S \cdot L$ (right).

points. The closed loop nominal system is stable when the open loop model is minimum phase. A linear continuous time system is minimal phase when all poles and zeros are in the left-hand plane. From the pole−zero map plotted in Figure 7 it can be concluded that this is not the case. As a result, nonlinear control techniques such as IOL and GMC are not used for the comparison study in this article.

Multivariable Controller Synthesis: LSDP. The design of a diagonal PI structure after selecting a pairing leads to a suboptimal design. In addition, the LQG/LQR controller has no guaranteed stability margin, which possibly leads to problems in case of model uncertainties. The following two advanced controller synthesis methods were used in order to obtain a robust controller: loop shaping design procedure (LSDP) and the μ-synthesis procedure. Both methods were successfully applied for controller synthesis for a binary distillation column.[22] However, in contrast to the approach of Gu, the inventory control and regulatory control problems are solved simultaneously in this work. By carrying out the H_∞ loop shaping design procedure—performed in Matlab using the command *ncfsyn*—the plant is shaped with a precompensator ($\mathbf{W}_1$) and a postcompensator ($\mathbf{W}_2$) that is the identity matrix. $\mathbf{W}_1$ is a diagonal matrix with the following transfer function on the diagonal (for $i = 1, ..., 0.5$):

$$\mathbf{W}_1(i,i) = 2\frac{s+1}{10s} \tag{7}$$

The value of 2 is chosen for the gain of the filter, in order to ensure a small steady-state error. Larger gains lead to smaller steady-state errors but worse transient response.[22] In addition, for larger values the closed loop system is unstable in the presence of the measurements noise and time delay. Figure 8 shows the frequency response of the plant G and the shaped plant G_s, respectively. Figure 9 plots the sensitivity function S and the complementary sensitivity function ($T = S \cdot L = S \cdot GK$), for 15 realizations of the described "multiplicative uncertainty model" consisting of a gain uncertainty and delay uncertainty.

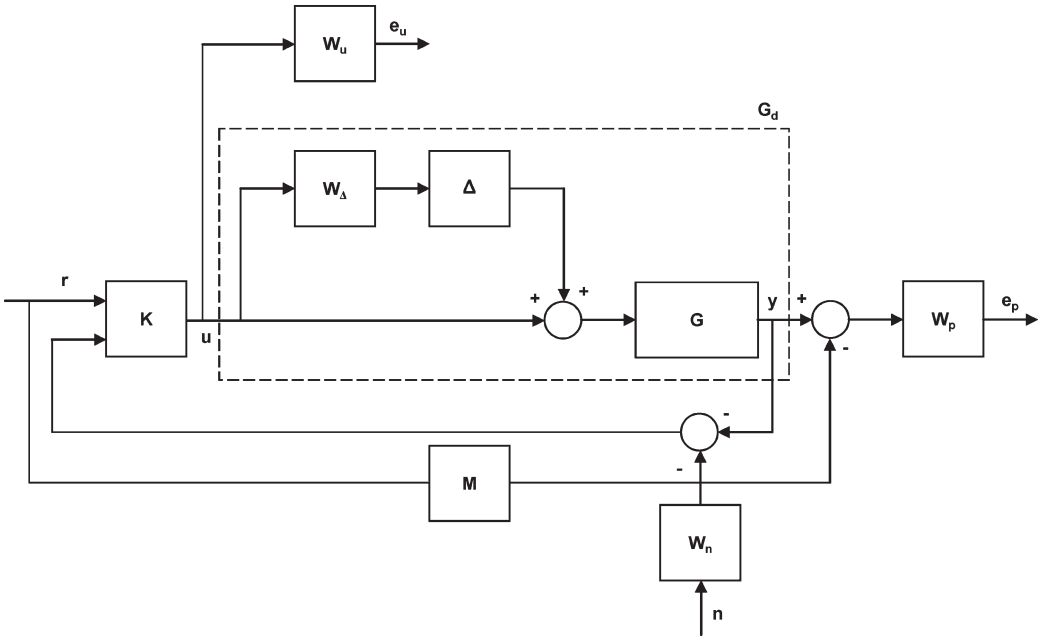

Figure 10. Closed loop interconnection structure of the DWC system with weighted outputs. The dashed box represents a plant G_d from the uncertainty set.

The structured value μ has a maximum of 0.7686. Hence, the closed loop system is stable with respect to the modeled uncertainty. The closed loop system and the weightings, shown in Figure 10,[22] are described hereafter.

Multivariable Controller μ-Synthesis (D-K Iteration Procedure). The linear model plant G is expanded with input multiplicative uncertainty to obtain a disturbed plant G_d. The input disturbance is an uncertain gain combined with an uncertain delay:

$$\mathbf{W}_u = \begin{pmatrix} k_1 e^{-\Theta_1 s} & & \\ & \ddots & \\ & & k_1 e^{-\Theta_1 s} \end{pmatrix} \tag{8}$$

where $k_i \in [0.8,1.2]$ and $\Theta_i \in [0,1]$ for $i = 1, ..., 5$. The matrix $\mathbf{W}_u$ can be split into two matrices:

$$\mathbf{\Delta} = \begin{pmatrix} \Delta_1 & & \\ & \ddots & \\ & & \Delta_5 \end{pmatrix} \qquad \mathrm{W}_\Delta = \begin{pmatrix} W_{\Delta_1} & & \\ & \ddots & \\ & & W_{\Delta_5} \end{pmatrix} \tag{9}$$

where $|\Delta_i| \leq 1$ for $i = 1, ..., 5$. The functions in the matrix $\mathbf{W}_\Delta$ are obtained via a fitting procedure in the frequency domain (Gu, 2005):[22]

$$W_{\Delta_i} = \frac{2.2138s^3 + 15.9537s^2 + 27.6702s + 4.0950}{1s^3 + 8.3412s^2 21.2393s + 22.6705} \qquad i = 1, ..., 5 \tag{10}$$

This function is the upper bound of 200 realizations of the relative uncertainty. Hence, an uncertainty set consisting of plants G_d is obtained, while the parameters of the uncertainty are within certain ranges. The next step is to synthesize a controller K that remains stable for all the plants G_d in the uncertainty set (*robust stability*). Robust performance is guaranteed if the structured singular value μ of the closed loop transfer function satisfies at each frequency the following condition:

$$\mu_{\hat{\Delta}}(F_L(P,K)(j\omega)) < 1, \quad \forall\omega \tag{11}$$

The D-K iteration searches for a controller that satisfies the above condition and stabilizes the closed loop system for all plants in the uncertainty set. The performance weighting function is a diagonal matrix with wp on the diagonal:

$$\mathbf{W}_p = \begin{pmatrix} \mathrm{wp} & 0.03 & \cdots & \cdots & 0.03 \\ 0.03 & \mathrm{wp} & 0.03 & & \vdots \\ \vdots & 0.03 & \mathrm{wp} & 0.03 & \vdots \\ \vdots & & 0.03 & \mathrm{wp} & 0.03 \\ 0.03 & \cdots & \cdots & 0.03 & \mathrm{wp} \end{pmatrix} \qquad \mathrm{wp} = 0.1\frac{s+3}{s+10^{-4}} \tag{12}$$

The off-diagonal elements are 0.03, such that the products and liquid levels will go to their prescribed set points. The function wp has the effect that for a low frequency range the set points are achieved. The functions $\mathbf{W}_u$ limit the control action over the frequency range $\omega \geq 150$ and the gains are chosen independently, such that in the case of strong measurement noise oversteering is avoided. This results in

$$\mathbf{W}_u = \begin{pmatrix} \mathrm{wu}_1 & & & & \\ & \mathrm{wu}_2 & & & \\ & & \mathrm{wu}_3 & & \\ & & & \mathrm{wu}_4 & \\ & & & & \mathrm{wu}_5 \end{pmatrix} \qquad \mathrm{wu}_i = g_i\frac{s+1}{s+1}$$
$$i = 1, ..., 3; \quad \mathrm{wu}_i = g_i\frac{s+1}{0.01s+1} \quad i = 4{-}5 \tag{13}$$

The weights g_i are chosen to ensure good performance and robust control: $g_1 = g_2 = g_3 = 10.44$ and $g_4 = g_5 = 0.2175$. The measurement noise on the five measurements is filtered by

$$\mathbf{W}_n = \begin{pmatrix} \mathrm{wn} & & & & \\ & \mathrm{wn} & & & \\ & & \mathrm{wn} & & \\ & & & \mathrm{wn}_4 & \\ & & & & \mathrm{wn}_5 \end{pmatrix} \qquad \mathrm{wn} = 0.01\frac{s}{s+1},$$
$$\mathrm{wn}_4 = \mathrm{wn}_5 = 0.2\frac{s}{s+1} \tag{14}$$

The reference is linked to the output of the plant G_d via a model M. The model is represented by a diagonal matrix with zero off-diagonal elements and the following transfer functions (wm) on the diagonal:

$$\mathrm{wm} = \frac{1}{1080s^2 + 288s + 1} \tag{15}$$

The off-diagonal elements are zero to avoid interaction and the constants are chosen such that the settling time after an impulse is ~1500 min. Inclusion of such a model makes it easier to achieve desired dynamics. The μ-synthesis (D-K iteration procedure)—performed in Matlab using the command *dksyn*—results in the iteration steps listed in Table 2.

Robust stability analysis reveals that the maximum value of μ is 0.3629. Hence the system is stable under perturbations that satisfy $\|\mathbf{\Delta}\| < 1/0.3629$. Likewise the maximum value of μ in the case of the robust performance analysis is 0.9847. Hence the system achieves robust performance for all the specified uncertainties.

6. Results and Discussion

In the dynamic simulations performed in this study, disturbances of +10% in the feed flow rate (F) and +10% in the feed composition (x_A) were used, as these are among the most significant ones at the industrial scale. Note that persistent disturbances give a better insight into the quality of the controller than zero-mean disturbances, as typically after a temporary disturbance the product compositions return to their given set points. However, the reflux and reboiler levels are unstable and need to be stabilized. For the PI controllers of the four investigated structures the tuning parameters (proportional gain and integral term) listed in Table 3 were used, along with the control loop direction.

The dynamic simulations were carried out in Mathworks Matlab combined with Simulink. The equations of the model are a system of ordinary differential equations that are solved using ODE15s solver available in Matlab. The relative tolerance (10^{-6}) and absolute tolerance (10^{-9}) make sure that the obtained solutions are reliable. Consequently, the time steps used by the solver are variable. Moreover, at any time step, the new input to the controller results in a new control signal. As shown next by the dynamic simulations, all PI control structures cope well with persistent disturbances. However, the control structures DV/

Table 2. Results of Multivariable μ-Synthesis (D-K Iterative Procedure)

iteration	controller order	max value of μ	achieved γ
1	194	14.4	16.1
2	204	1.4	1.5
3	218	0.985	1.038

Table 3. Tuning Parameters of PI Controllers

DB/LSV	P (%/%)	I (min)	D (min)	control direction
$x_A \rightarrow L$	3	80	0	+
$x_B \rightarrow S$	3	80	0	−
$x_C \rightarrow V$	3	80	0	+
tank level $\rightarrow D$	0.5	100	0	−
reboiler level $\rightarrow B$	0.5	100	0	−
DV/LSB	P (%/%)	I (min)	D (min)	control direction
$x_A \rightarrow L$	1	100	0	+
$x_B \rightarrow S$	1	100	0	−
$x_C \rightarrow B$	1	100	0	−
tank level $\rightarrow D$	0.1	400	0	−
reboiler level $\rightarrow V$	0.1	400	0	−
LB/DSV	P (%/%)	I (min)	D (min)	control direction
$x_A \rightarrow D$	3	75	0	−
$x_B \rightarrow V$	3	75	0	+
$x_C \rightarrow S$	3	75	0	+
tank level $\rightarrow L$	0.5	400	0	−
reboiler level $\rightarrow B$	0.5	400	0	−
LV/DSB	P (%/%)	I (min)	D (min)	control direction
$x_A \rightarrow D$	1	100	0	−
$x_B \rightarrow S$	1	100	0	−
$x_C \rightarrow B$	1	100	0	−
tank level $\rightarrow L$	0.5	400	0	−
reboiler level $\rightarrow V$	0.5	400	0	−

Table 4. Settling Time to Reach Steady State for Different Persistent Disturbances

	settling time (min)	
control structure	+10% feed flow rate	+10% x_A in feed
DV/LSB	≫1000	≫1000
LV/DSB	≫1000	≫1000
LB/DSV	790	561
DB/LSV	714	525
LQR/LGQ (integral action)	510	839
LQR/LGQ (feed forward)	432.5	N/A
LSDP	645	569
μ-controller	642	569

LSB and LV/DSB make the DWC return to steady state only after a long time (>1000 min).

The LQG controller with feed-forward control has only good results for (persistent) disturbances in the feed flow rate. For other disturbances the tuning of the feed-forward terms is less straightforward. The controller has no feedback on the error term that is the difference of the set points and the measured values. As a result, offset in the product purities appears. To solve this problem, the LQG controller is combined with an integral term.

A stop criterion is used for all test cases in order to have a fair comparison of the controllers: the simulation is stopped if the condition $\|(x_A,x_B,x_C) - (0.97,0.97,0.97)\|^2 < 1e^{-10}$ holds at time t_1 and also holds at time $t_2 = t_1 + 40$ min, where $t_1 < t_2$. The resulting times (smaller values mean better control) are shown in Table 4.

The effect of measurement noise on the control performance was also investigated. At the five measurements, filtered white noise was added using the following filter that should be determined according to the spectral contents of the sensor noises accompanying the measurements of the product purities and the liquid levels.[22]

$$\text{filter} = 0.01\frac{s}{s+1} \tag{16}$$

Hence for frequencies $\omega > 1$ the damping is 0 dB and for $\omega \leq 1$ there is a damping of 20 dB per decade. The gain $f_{gain} = 0.01$ for the composition channels and 0.2 for the tank and reboiler level sensor, respectively, and the noise source is a block signal with mean 1 and sample time 0.1 min. Consequently, the gain was selected to be 1% of the nominal measured value.

After a constant load disturbance in the feed at first instance all product purities decrease (Figure 11, left), but then the top and bottom purities decrease significantly while the middle product purity increases. The product flow rates D and B are steered by the controller above the new nominal values in order to stabilize the product purities. The composition load disturbance is handled faster and there is no serious overshoot (Figure 11, right). The maximum difference between the set points and the measured product purity in the case of feed flow rate disturbance is between 0.015 and 0.020, and approximately 0.008 in the case of feed composition disturbance.

Unlike the previous PI control structure, DV/LSB needs a long period to stabilize the plant around the new steady state (Figure 12, left). The overshoot in the purity of x_A in the case of feed composition disturbance is large: approximately 0.08 (Figure 12, right).

The PI control structure LB/DSV controls the DWC in a time scale similar to DB/LSV (Table 4). The disturbances resulting from the changes in the nominal feed are controlled away, showing only a small overshoot in the product purities: less than 0.02 for both cases (Figure 13).

The control structure of the LV/DSB configuration is such that there are amplifying effects due to the outcome of the control action of both inventory and regulatory control. As a result, the feed flow rate disturbance leads to an increase of L_0 and V_0 to maintain the demanded tank and reboiler levels. Consequently, the product purities increase and the levels of the tank and reboiler drop very quickly due to the synergy effect of the inventory and regulatory control (Figure 14, left). This phenomenon is also present for the composition load but less strongly (Figure 14, right). Nevertheless the steady state can only be reached after a long time and the feed flow rate disturbance leads to an error of 0.05 in the purity of product B. In addition, compared to the three previous control structures, relatively high flow rates are used to control the DWC: $L_0 > 1.1$ and $V_0 > 1.3$.

Figure 15 shows the RGA number vs frequency plot. This clearly distinguishes between the LV/DSB and DB/LSV control structures, where the DB/LSV option is preferable to LV/DSB. However, the RGA numbers for the other structures (LB/DSV and DV/LSB) have similar values, located in between the RGA numbers of the LV/DSB and DB/LSV structures.

Nevertheless, there is a performance discrepancy that can be explained by investigating the absolute RGA matrix at $s = 0.0392$ (eq 17) and conclude that the pairing x_A−V and x_B−V is more effective than x_B−L and x_C−L. Similar behavior is expected for other frequencies. From the multiloop structure with the best RGA number (DB/LSV) we can obtain LB/DSV or DV/LSB via two permutations of the input variables, respectively. As a result, the variable V for controlling H_R has a bad impact on the product compositions, worse than the case where L is used for controlling H_T in the LB/DSV configuration.

$$|\text{RGA}| = \begin{pmatrix} 1.0360 & 0.0019 & 0.1509 & 0 & 0 \\ 0.9283 & 0.6016 & 0.4661 & 0 & 0 \\ 0.8753 & 0.4789 & 1.3645 & 0 & 0 \\ 0 & 0 & 0 & 1 & 0 \\ 0 & 0 & 0 & 0 & 1 \end{pmatrix} \tag{17}$$

While the LQG controller results in optimal state feedback in the case of zero-mean noise, problems occur in the case of

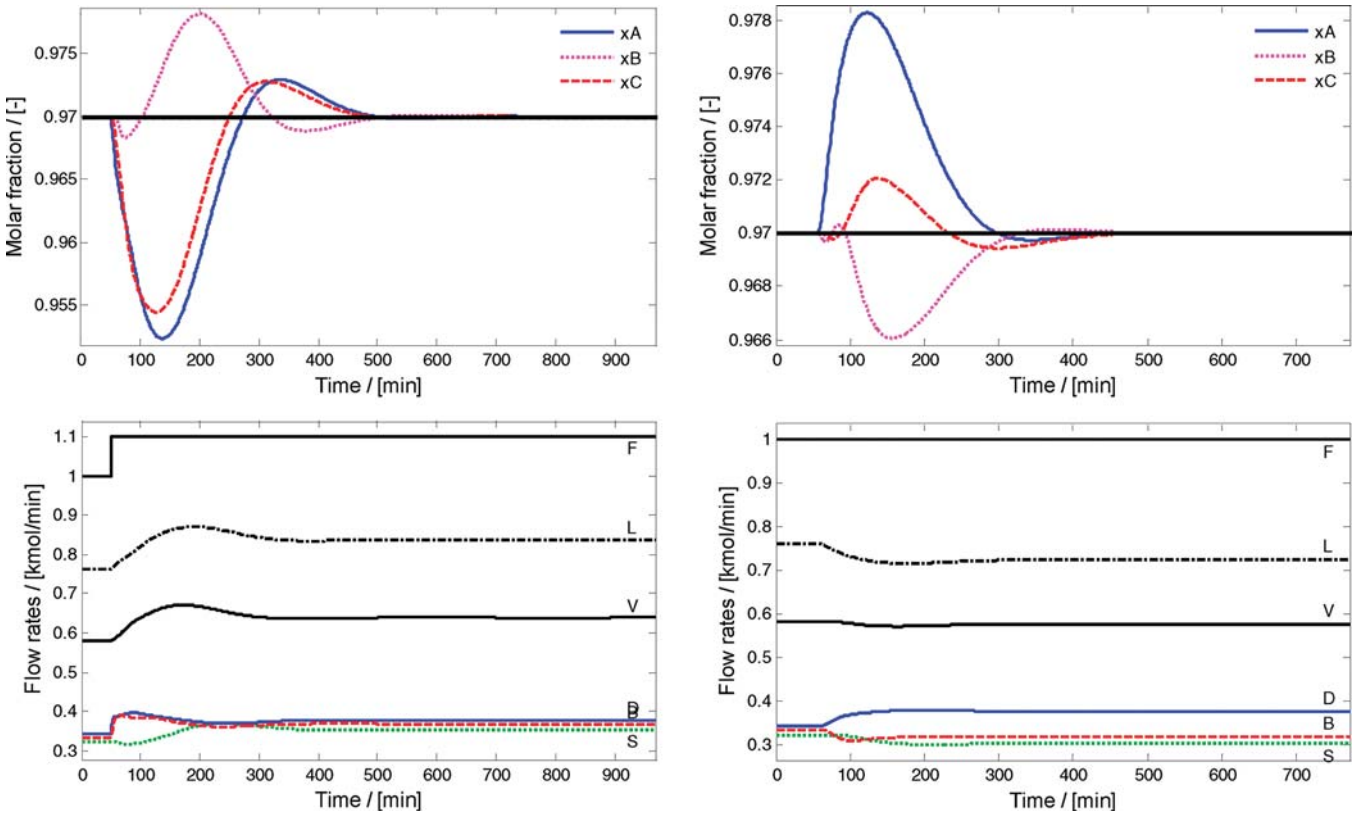

Figure 11. Dynamic response of the DB/LSV control structure, at a persistent disturbance of +10% in the feed flow rate (left) and +10% x_A in the feed composition (right).

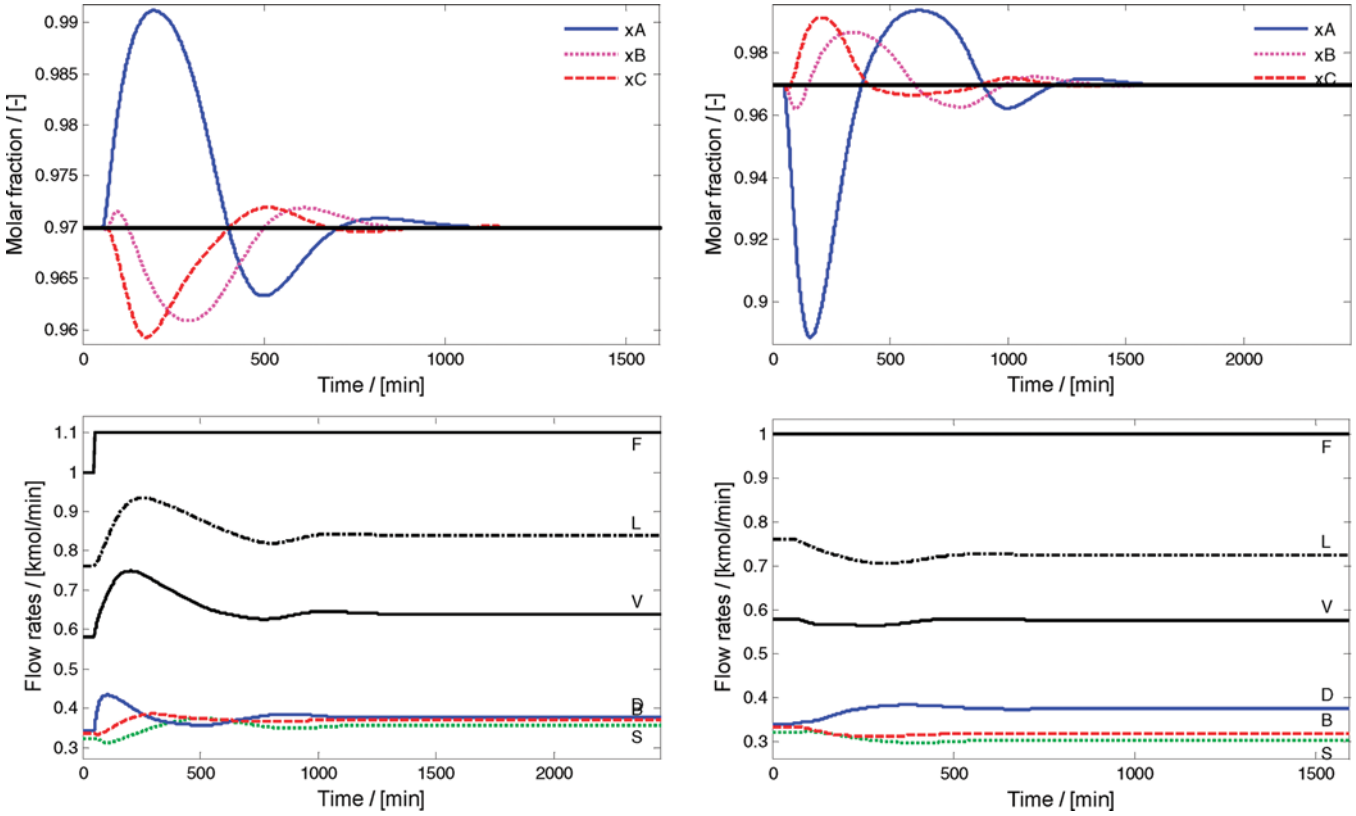

Figure 12. Dynamic response of the DV/LSB control structure, at a persistent disturbance of +10% in the feed flow rate (left) and +10% x_A in the feed composition (right).

persistent disturbance. Hence, the LQG controller needs to be expanded in order to handle the load disturbances. Combined with the feed-forward controller, the feed flow rate disturbance can easily be controlled and results in a small settling time (Figure 16, left). In the case of composition disturbance there is no clear relationship between the amount of input and

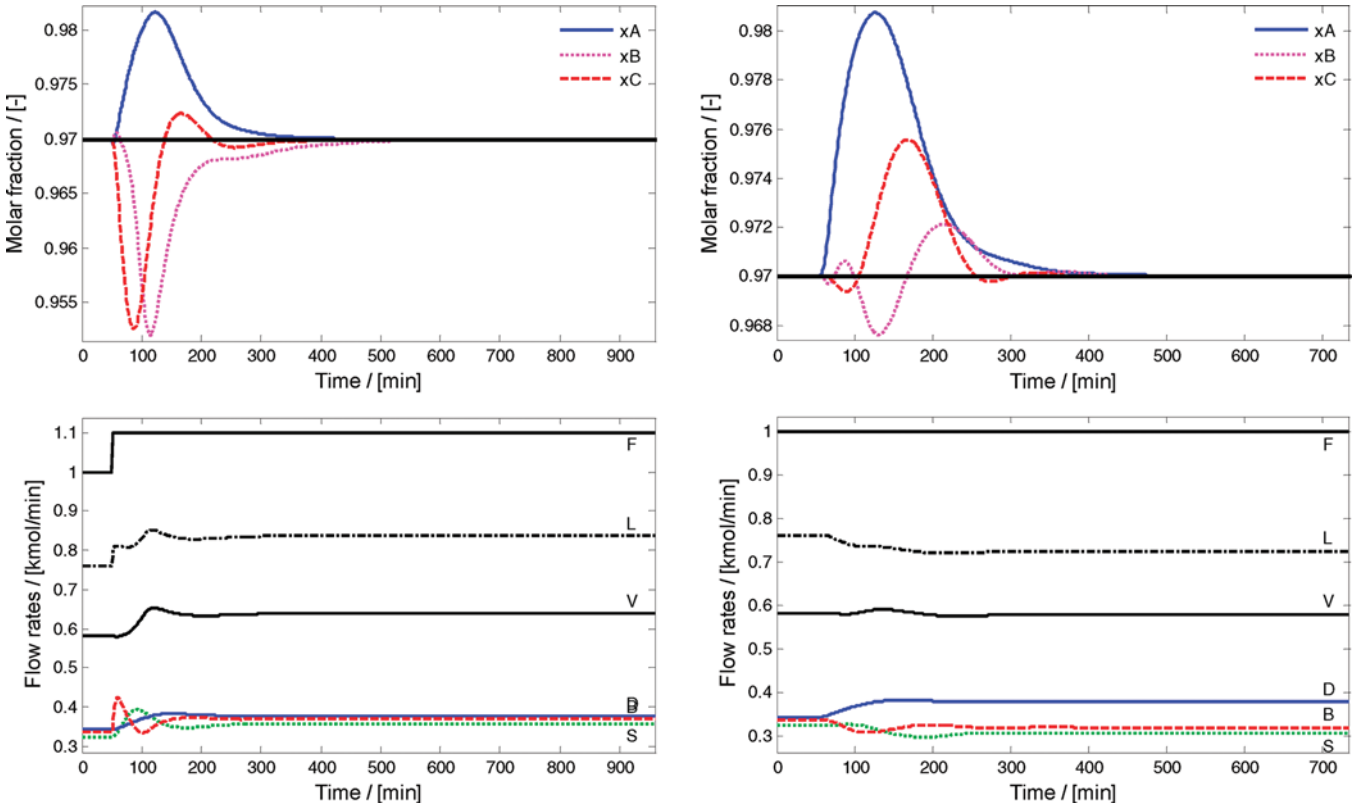

Figure 13. Dynamic response of the LB/DSV control structure, at a persistent disturbance of +10% in the feed flow rate (left) and +10% x_A in the feed composition (right).

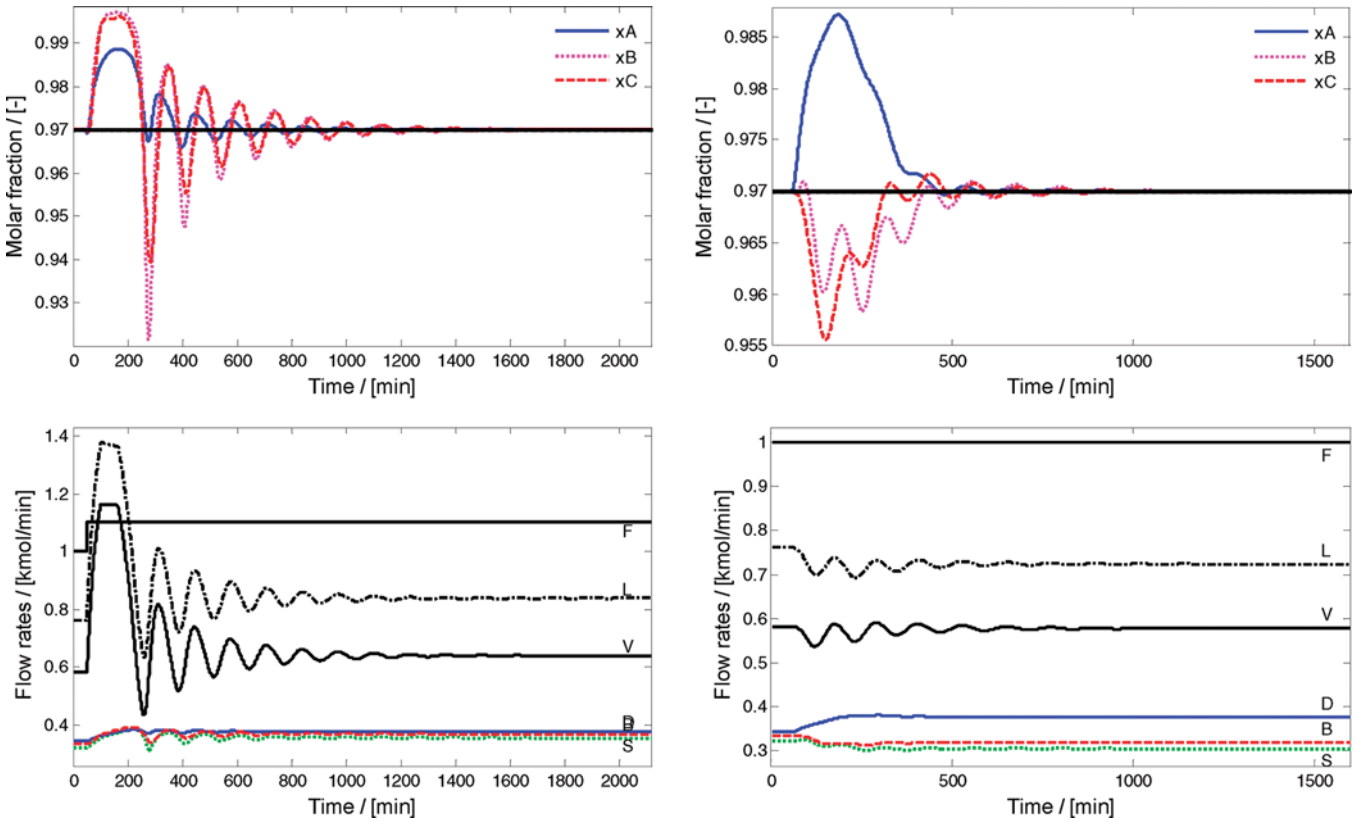

Figure 14. Dynamic response of the LV/DSB control structure, at a persistent disturbance of +10% in the feed flow rate (left) and +10% x_A in the feed composition (right).

output—as it was for flow rate—hence the feed forward leads to bad control resulting in a different steady-state error (Figure 16, right).

The LQG combined with an integral action stabilizes the column around the demanded set points for all the disturbances (Figure 17). In both cases the maximum error in the product

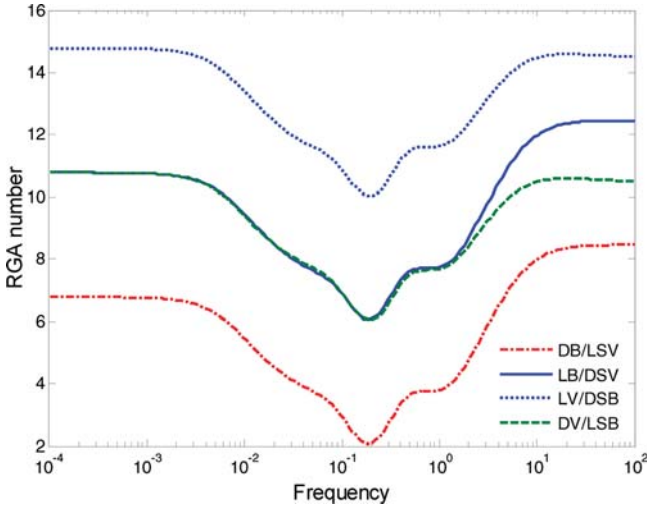

Figure 15. RGA number vs frequency, for the PID loops within a multiloop framework.

compositions is less than 0.005. Furthermore, there is a striking contrast between settling time after a feed flow rate disturbance and a feed composition disturbance: in the latter case the settling time is much longer.

The controller obtained by the LSDP (of order 164) is implemented, and the results are shown in Figure 18. The application of this advanced controller leads to significantly shorter settling times than the best PI control structures. Remarkably, the maximal offset error in the product compositions is less than 0.002.

Figure 19 shows that the μ-controller (of order 218) is able to steer the system to the desired steady state after persistent disturbance. Similar to the LSDP controller, the settling time is significantly shorter compared to the PI control structures. Also, the maximal error in the product compositions is less than 0.002. Moreover, the settling time of the system controlled by the μ-controller is the smallest of all compared control structures.

In addition to the previous scenarios, noise and a time delay of 1 min were added to each measurement channel. The added measurement noise is filtered using the filter described by eq 16. This simulation was carried out only for the PI control structure DB/LSV, LQG with integral action, LSDP controller, and the μ-controller as these controllers lead to the shortest settling times. The impact of noise and delay on the LB/DSV PI structure is expected to be comparable with that on DB/LSV. The dynamic simulation of the PI control structure DB/LSV with measurement noise is shown in Figure 20.

The regulatory part of the control structure (DB) is controlling the tank level and the reboiler level. The measurement noise has more impact on the flow rates D and B than the other three flow rates (Figure 20, right). In addition, the persistent disturbance results in a serious offset for $t < 500$ min. However, the control structure is robust to the measurement noise and time delays.

In order to have a fair comparison with the PI control structure, the scales on the Y-axis are the same. The results for the LQG with integral action control structure (Figure 21) shows similar chaotic behavior in the product composition compared with the PI control structure. Nevertheless, the maximal deviation in the product composition is less than 0.008 and the persistent disturbance is no longer visible after approximately $t > 200$ min. While the weighting of the integral error for the product compositions is much larger compared to the liquid levels, the noise has more impact on the control signals L_0, V_0, and S. In addition, the input weightings are also different: the weightings on L_0 and V_0 are larger than the weighting on S,

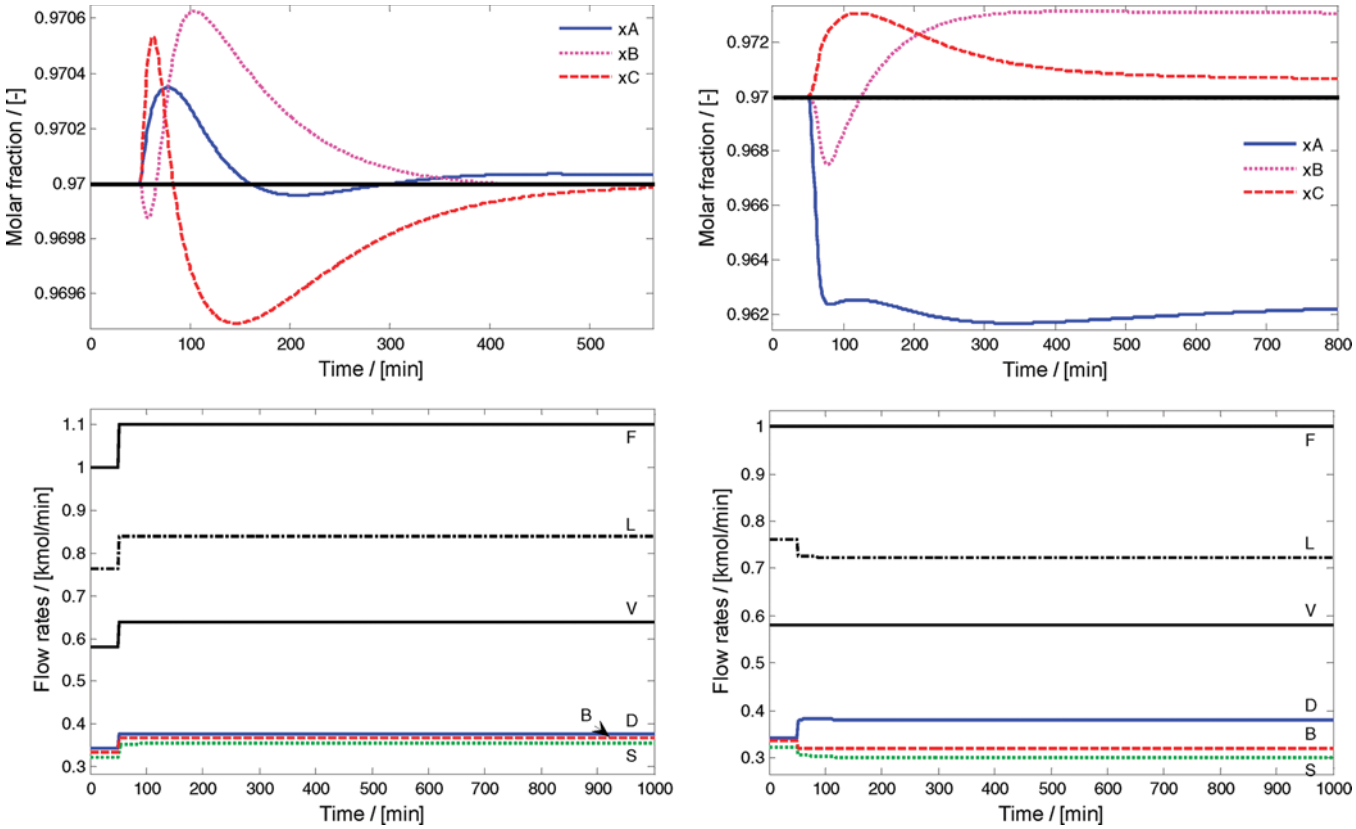

Figure 16. Dynamic response of LQG controller with feed forward, at a persistent disturbance of +10% in the feed flow rate (left) and +10% x_A in the feed composition (right).

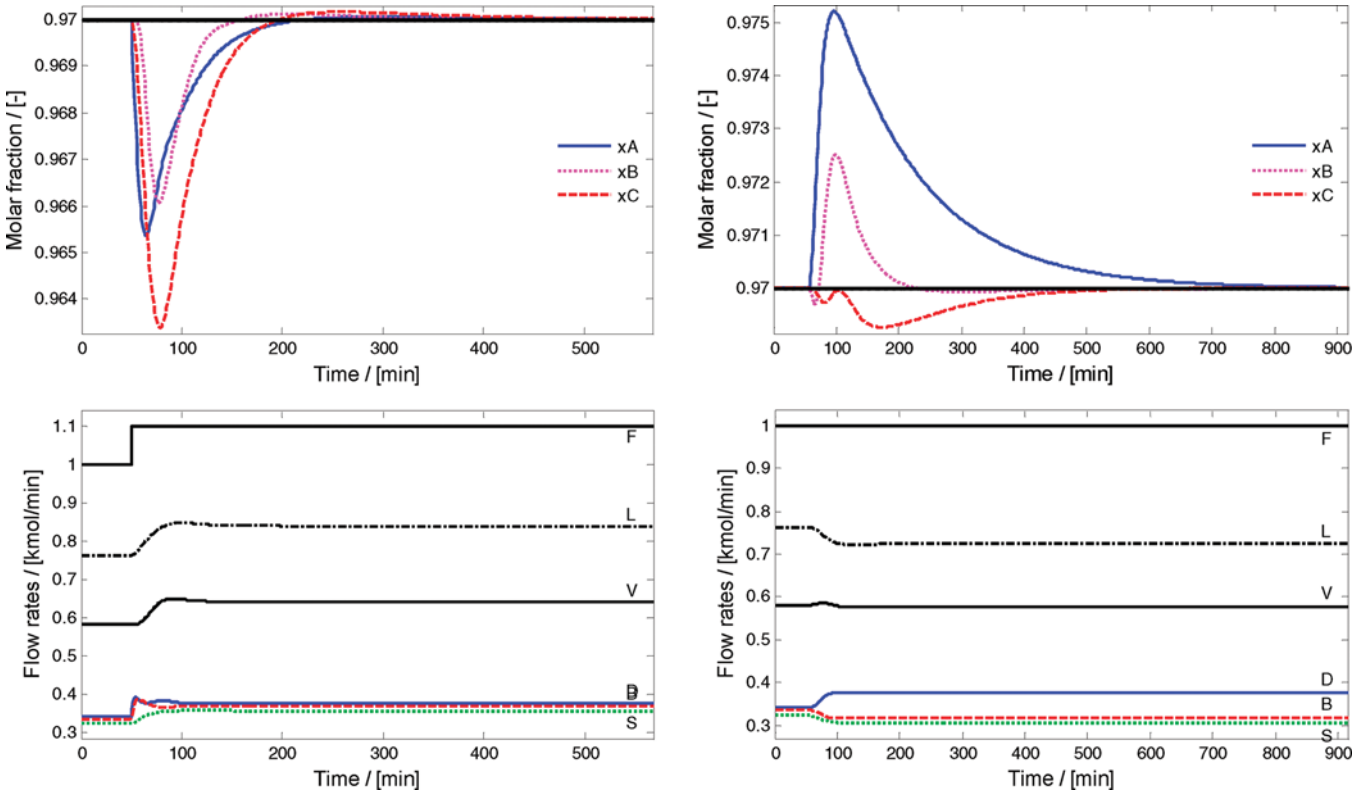

Figure 17. Dynamic response of LQG combined with integral action control structure, at a persistent disturbance of +10% in the feed flow rate (left) and +10% x_A in the feed composition (right).

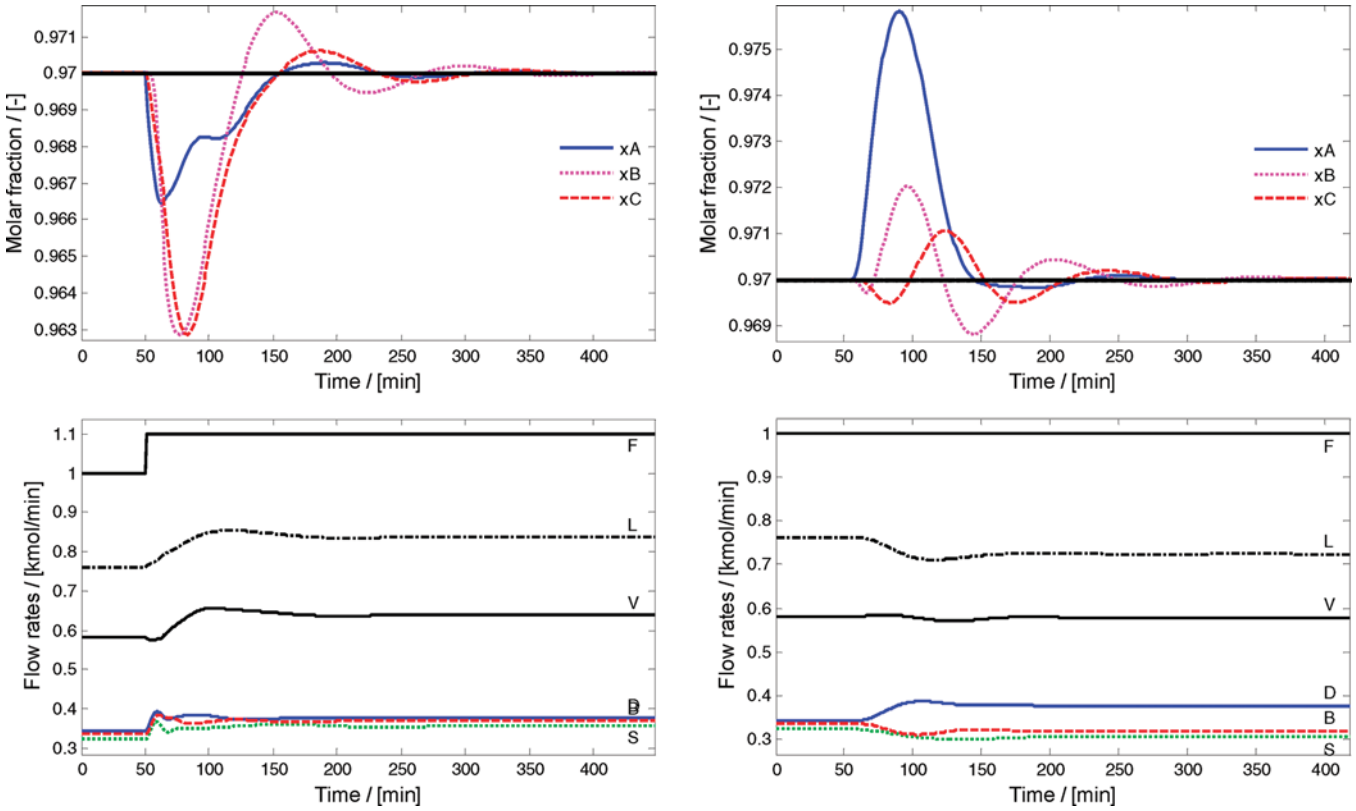

Figure 18. Dynamic response of the LSDP controller, at a persistent disturbance of +10% in the feed flow rate (left) and +10% x_A in the feed composition (right).

and the weighting on *S* is larger than the weightings on *B* and *D*. Hence, there is a trade-off in a fast control action and measurement noise reduction.

The high order LSDP controller is more sensitive to noise as shown by the chaotic behavior of the product purities plotted in Figure 22. The closed loop remains stable, but when

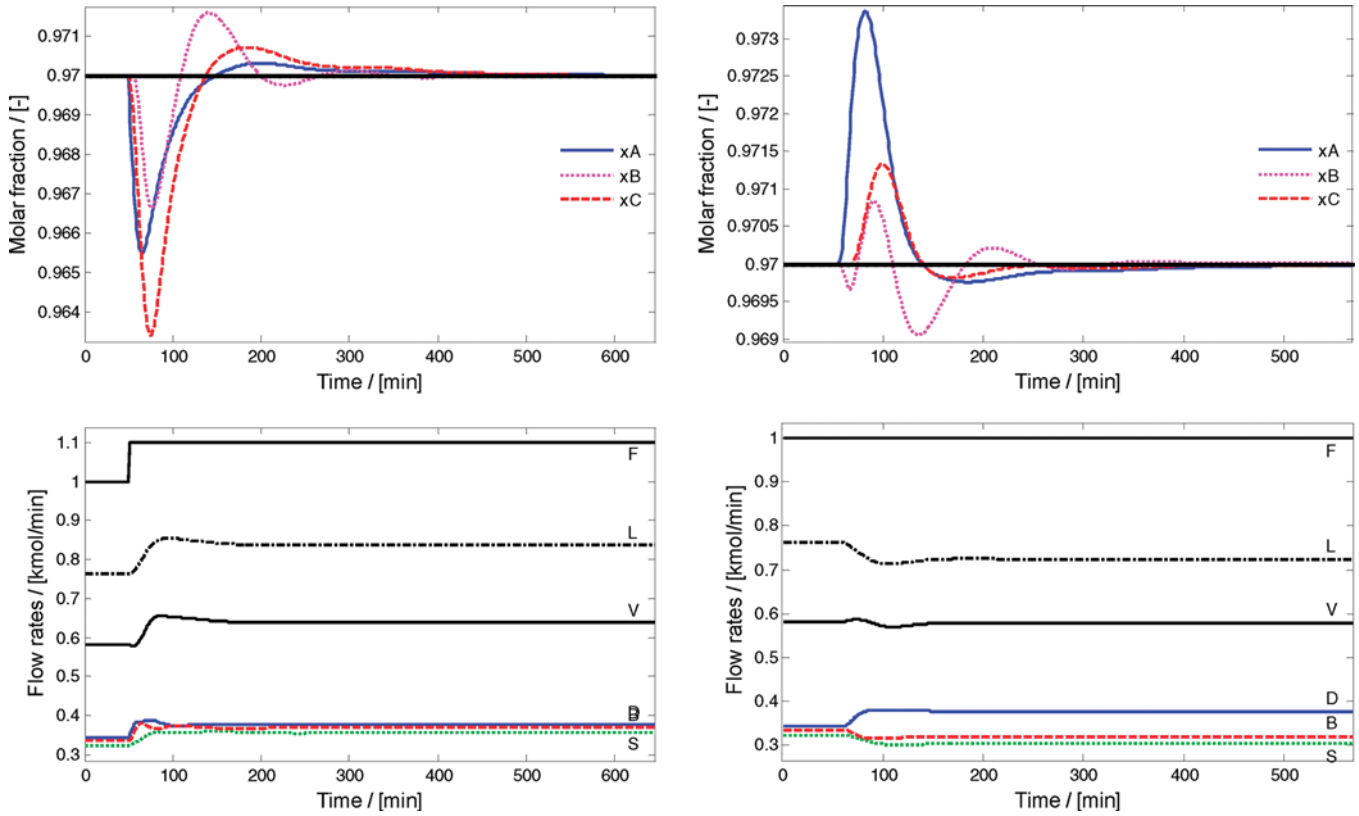

Figure 19. Dynamic response of the μ-controller, at a persistent disturbance of +10% in the feed flow rate (left) and +10% x_A in the feed composition (right).

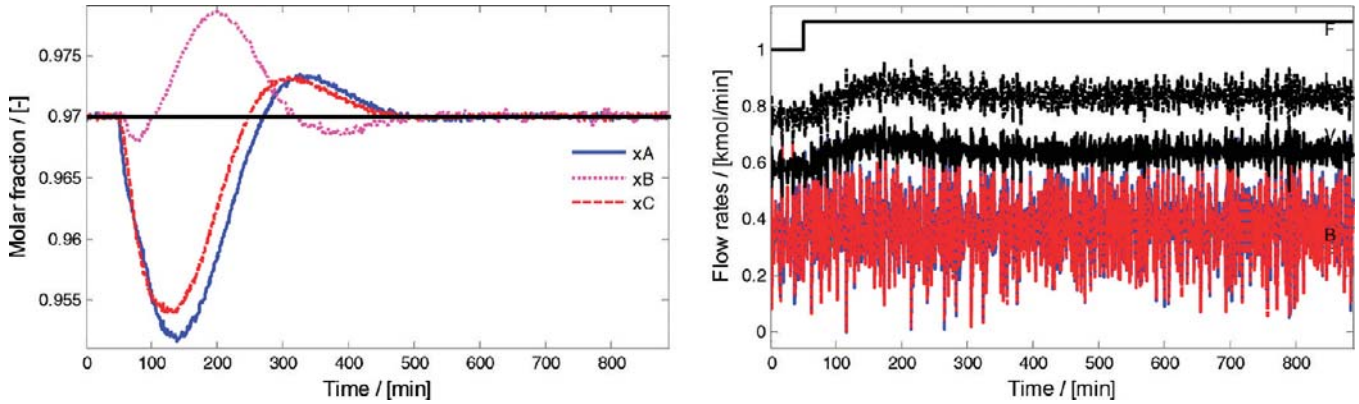

Figure 20. Dynamic response of the DWC with the DB/LSV control structure, at a persistent disturbance of +10% at $t = 50$ min in the feed flow rate while there is white measurement noise and a time delay.

synthesizing the controller, the noise source is not taken into account. In the absence of measurement noise the control action is such that the settling time is short.

The effect of measurement noise and delay on the system controlled by the μ-controller is shown in Figure 23. While there is chaotic behavior in the product compositions, the control actions are very calm despite the present noise. Also, the maximum deviation in the product composition is small—less than 0.008.

Note that all the control structures investigated were tested for a large number of disturbances, but here we limit to only the ones that are relevant at the industrial scale. Although the reported disturbances are not exerted at the same time, no serious problems—such as instability or lack of capability to reach the set points—were observed in the case of simultaneous disturbances. The same holds for a decrease of 10% in the feed flow rate or feed composition. The exerted noise is filtered and the gain is approximately 1% of the nominal value on the channel. In an industrial case the filter should correspond to the measurement sensor. Moreover, there is a need to consider the dynamics of the actuators (e.g., time constants, stiction) in evaluating the controller performance.[41,42] However, for the DWC studied in this work, the time scale of the changes in product purities and liquid levels is in minutes—hence the neglection of the actuator time constant and stiction is expected to be realistic.

Remarkably, PI control structures already for a long time have been the celebrated controllers in the chemical industry.[38] Several reasons are given for their success: (1) simplicity of the control structure; (2) robustness with respect to model

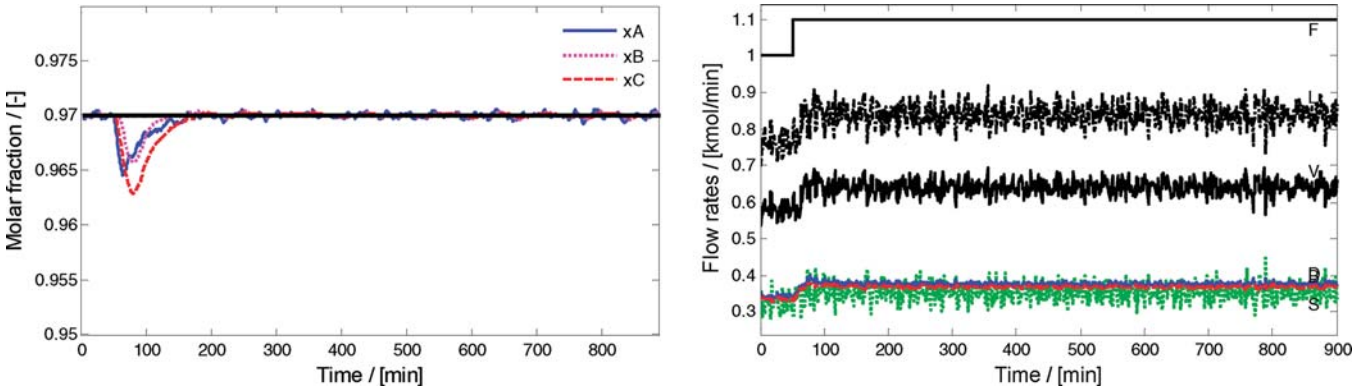

Figure 21. Dynamic response of the DWC with the LQG with integral action control structure, at a persistent disturbance of +10% at $t = 50$ min in the feed flow rate while there is white measurement noise and a time delay.

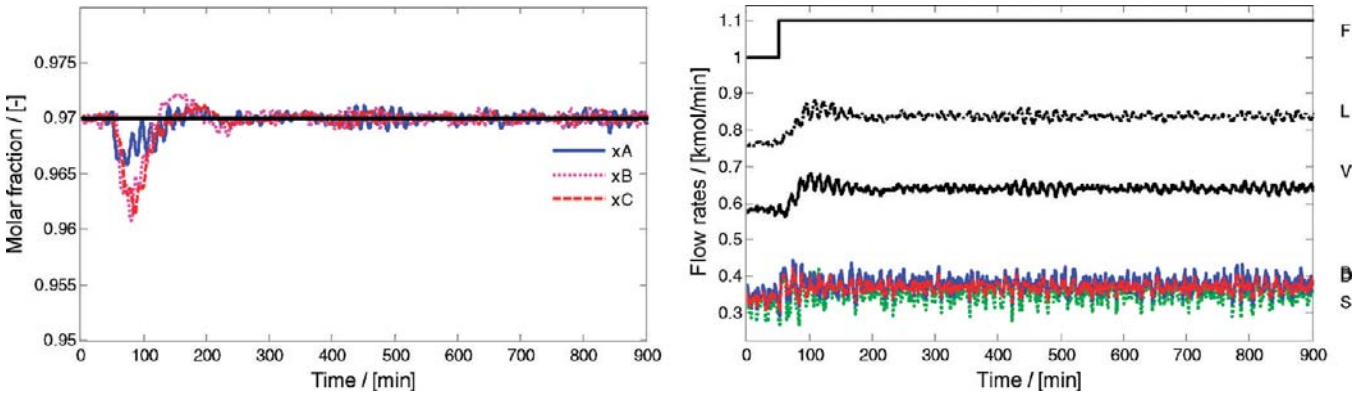

Figure 22. Dynamic response of the DWC with the LSDP controller, at a persistent disturbance of +10% at $t = 50$ min in the feed flow rate while there is white measurement noise and a time delay.

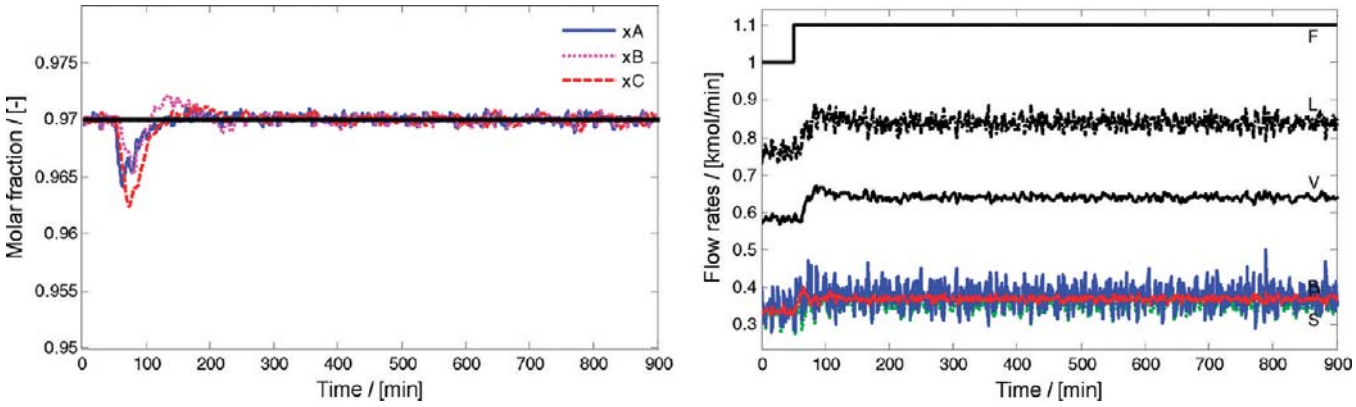

Figure 23. Dynamic response with the μ-controller, at a persistent disturbance of +10% at $t = 50$ min in the feed flow rate while there is white measurement noise and a time delay.

uncertainties and disturbances; (3) relatively easy manual stabilization of the process with PID loops within a multiloop framework, when an actuator or sensor fails.

The LQG control structure offers optimal state estimation and an optimal control with respect to the cost function (eq 5), providing that the matrices **Q** and **R** are chosen in an appropriate way. Unlike LQG, many control variables have to be chosen for the PID loops within a multiloop framework. In addition, the LQG control structure guarantees stability of the closed loop system consisting of a linearized DWC, whereas the stability problem of the PID loops within a multiloop framework is still open.[38] The full model is nonlinear, and the optimal state estimation and optimal control holds only for the linearized model. However, as shown by Figure 4, this should not lead to problems. Moreover, the dynamic simulations showed no control or stability problems of the closed loop system. Furthermore, there is a trade-off between a short settling time in the case of no measurement delay and noise, and a very smooth control action in the case of measurement noise. A short settling time results in a more chaotic control if noise is present.

The LSDP controller has difficulties coping with the measurement noise, while the μ-controller has the shortest settling times and a relatively good behavior when measurement noise and delay are present. Unlike the μ-controller, controller reduction of the LSDP controller leads to serious problems in the presence of measurement noise and delay. As a result, the computer needs much more time to carry out a simulation of

the DWC controlled by a LSDP controller compared with the other control structures.

In addition to the controllers compared in this work, model predictive control (MPC) is an important candidate for controlling nonlinear processes. Efficient implementations of nonlinear MPC in industrial cases were already reported for several nonlinear processes[43−47] and in particular DWC.[29] However, more advanced controllers such as MPC are beyond the scope of the current study.

7. Conclusions

The comparison of control strategies performed in this work—based on a dividing-wall column separating the ternary mixture benzene−toluene−xylene—provides significant insight into the controllability of DWC, and gives important guidelines for selecting the appropriate control structure. The dynamic model of the DWC used in this study is not a reduced one, but is a full-size nonlinear model that is representative for industrial separations. Although the application of nonlinear based controllers is very appealing—since linearization is not necessary—the general model controller (GMC) is not applicable in practice for the DWC as the open loop model is not minimum phase.

Due to practical considerations based on the physical flows, there are basically four control strategies possible based on PID loops within a multiloop framework: DB/LSV, DV/LBS, LB/DSV, and LV/DSB. The results of the dynamic simulations show that DB/LSV and LB/DSV are the best control structures among the decentralized multivariable PI structured controllers, being able to handle persistent disturbances in reasonably short times. However, the DV/LBS and LV/DSB structures needed very long settling times, in the case of persistent disturbances.

The DWC model is not only nonlinear but also a true multiinput−multioutput (MIMO) system; hence the applicability of a MIMO control structure starting with a LQG controller was also investigated. With the LQG controller there is an optimal tuning with respect to the corresponding cost function. In order to cope with persistent disturbances, two options were explored: feed-forward control and addition of an integral action. The LQG combined with a feed forward has good results for a persistent disturbance in the feed flow rate. However, for changes in the feed composition and condition, it is difficult to find a good tuning. Moreover, persistent disturbances other than the ones used for tuning cannot be controlled with LQG. Nevertheless, combining LQG with an integral action and reference input solves the problem. Depending on the expected measurement noise, the cost function can be determined. Moreover, robustness against measurement noise results in a more conservative tuning.

The loop shaping design procedure (LSDP) used in this work leads to a feasible μ-controller that has some additional benefits, while specific model uncertainties can be incorporated in the control structure. However, reduction of the LSDP controller (of order 164) is not possible since the reduced controller is unable to control the column. In contrast, the μ-controller can be reduced from order 218 to only 25 and still have a good control performance. In the DWC case described here, the obtained μ-controller is able to minimize the settling time when handling persistent disturbances. While PI control structures are also able to control the DWC, significantly shorter settling times can be achieved using MIMO controllers. Moreover, persistent disturbances are also controlled faster using a MIMO controller.

Acknowledgment

We thank Karel Keesman (Wageningen University and Research Centre, The Netherlands) for helpful discussions, as well as Da-Wei Gu (Leicester University, U.K.) and Sigurd Skogestad (Norwegian University of Science and Technology) for technical support. The financial support given by AkzoNobel to R.C.v.D. during his internship and final M.Sc. project is also gratefully acknowledged.

Dynamic Model of DWC

The nonlinear model of the DWC is described by the following mathematical equations:

$$\dot{\mathbf{x}} = f(\mathbf{x}, \mathbf{u}, \mathbf{d}, t)$$
$$\mathbf{y} = g(\mathbf{x}) \tag{A.1}$$

where $\mathbf{u} = [L_0\ S\ V_0\ D\ B\ R_L\ R_V]$ and $\mathbf{d} = [F\ z_1\ z_2\ q]$. Furthermore, the state vector $\mathbf{x}$ consists of 104 compositions for the first two components and 52 liquid holdups. The output vector is given by $\mathbf{y} = [x_A\ x_B\ x_C\ H_T\ H_R]$.

State Equations. Numbering is from top to bottom starting in the prefractionator and then continuing in the main column. Overall, the DWC has six sections (S1−S6) that are clearly illustrated in Figure 2.

$$H_i \frac{dx_{i,j}}{dt} = L_{ij}(x_{\text{liquid\_split},j} - x_{i,j}) + V_{i-1,j}(y_{i-1,j} - y_i) \qquad i = 1 \tag{A.2}$$

$$H_i \frac{dx_{i,j}}{dt} = L_{ij}(x_{i+1,j} - x_{i,j}) + V_{i-1,j}(y_{i-1,j} - y_i) \qquad i = 2, ..., 8 \tag{A.3}$$

$$H_i \frac{dx_{i,j}}{dt} = L_{i,j}(x_{\text{in\_2},j} - x_{i,j}) + V_{i-1,j}(y_{i-1,j} - y_i) \qquad i = 9 \tag{A.4}$$

$$H_i \frac{dx_{i,j}}{dt} = L_{i,j}(x_{i+1,j} - x_{i,j}) + V_{i-1,j}(y_{i-1,j} - y_i) \qquad i = 10, ..., 16 \tag{A.5}$$

$$H_i \frac{dx_{i,j}}{dt} = L_{i,j}(x_{\text{in\_3},1} - x_{i,j}) + V_{i-1,j}(y_{i-1,j} - y_i) \qquad i = 17 \tag{A.6}$$

$$H_i \frac{dx_{i,j}}{dt} = L_{i,j}(x_{i+1,j} - x_{i,j}) + V_{i-1,j}(y_{i-1,j} - y_i) \qquad i = 18, ..., 23 \tag{A.7}$$

$$H_i \frac{dx_{i,j}}{dt} = L_{i,j}(x_{i+1,j} - x_{i,j}) + V_{i-1,j}(y_{\text{in\_3},j} - y_i) \qquad i = 24 \tag{A.8}$$

$$H_i \frac{dx_{i,j}}{dt} = L_{i,j}(x_{\text{in\_4},j} - x_{i,j}) + V_{i-1,j}(y_{i-1,j} - y_i) \qquad i = 25 \tag{A.9}$$

$$H_i \frac{dx_{i,j}}{dt} = L_{i,j}(x_{i+1,j} - x_{i,j}) + V_{i-1,j}(y_{i-1,j} - y_i) \qquad i = 26, ..., 32 \tag{A.10}$$

$$H_i \frac{dx_{i,j}}{dt} = L_{i,j}(x_{\text{in\_25},j} - x_{i,j}) + V_{i-1,j}(y_{i-1,j} - y_i) \qquad i = 33 \tag{A.11}$$

$$H_i \frac{dx_{i,j}}{dt} = L_{i,j}(x_{i+1,j} - x_{i,j}) + V_{i-1,j}(y_{i-1,j} - y_i) \qquad i = 34, ..., 40 \quad (A.12)$$

$$H_i \frac{dx_{i,j}}{dt} = L_{i,j}(x_{\text{in\_6},j} - x_{i,j}) + V_{i-1,j}(y_{i-1,j} - y_i) \qquad i = 41 \quad (A.13)$$

$$H_i \frac{dx_{i,j}}{dt} = L_{i,j}(x_{i+1,j} - x_{i,j}) + V_{i-1,j}(y_{i-1,j} - y_i) \qquad i = 42, ..., 48 \quad (A.14)$$

where the liquid holdup is given by

$$\frac{dH_i}{dt} = L_{i+1} - L_i \quad (A.15)$$

and the vapor composition is computed by

$$y_{i,j} = \frac{\alpha_j}{\sum_j \alpha_j x_{i,j}} \quad (A.16)$$

for the components $j \in \{1,2,3\}$ and relative volatilities α.

Furthermore, some special concentrations have to be specified:

$$x_{\text{in\_2},j} = (L_8 x_{8,j} + F_0 z_j - (1 - q)F_0 y_{9,j})/L_9 \qquad \text{input section 2; tray no. 9} \quad (A.17)$$

$$x_{\text{in\_1},j} = x_{\text{liquid\_split}} \qquad \text{input section 1; tray no. 1} \quad (A.18)$$

$$x_{\text{in\_4},j} = x_{\text{liquid\_split}} \qquad \text{input section 4; tray no. 25} \quad (A.19)$$

$$x_{\text{in\_6},j} = (L_{16} x_{16} + L_{40} x_{40})/x_{41} \qquad \text{liquid input section 6; tray no. 41} \quad (A.20)$$

$$y_{\text{in\_3},j} = (V_1 y_1 + V_4 y_{25})/V_{24} \qquad \text{vapor input section 3; tray no. 24} \quad (A.21)$$

$$x_{\text{in\_5},j} = x_{\text{side\_splitter}} \qquad \text{liquid input section 5, after liquid splitter} \quad (A.22)$$

Dynamics of Liquid Splitter. The liquid splitter is located between section 3 and sections 1/4.

$$\frac{d}{dt} H_{\text{liquid\_split}} = L_{24} - (L_1 + L_{25})$$

$$H_{\text{liquid\_split}} \frac{d}{dt} x_{\text{liquid\_split}} = L_{24}(x_{24} - x_{\text{liquid\_split}}) \quad (A.23)$$

Dynamics of Side Splitter. The liquid side splitter is located between section 3 and sections 4/5.

$$\frac{d}{dt} H_{\text{side\_split}} = L_{32} - L_{33} - S$$

$$H_{\text{side\_split}} \frac{d}{dt} x_{\text{side\_split}} = L_{32}(x_{32} - x_{\text{side\_split}}) \quad (A.24)$$

Dynamics of Reboiler. This is situated between section 3 and sections 1/4.

$$\frac{d}{dt} H_{\text{reboiler}} = L_6 - V_0 - B$$

$$H_{\text{reboiler}} \frac{d}{dt} x_{\text{reboiler}} = L_{\text{in}}(x_{\text{in}} - x_{\text{reboiler}}) - V_0(y_{\text{reboiler}} - x_{\text{reboiler}}) \quad (A.25)$$

Dynamics of the Reflux Tank. This is situated between section 3 and sections 4/5.

$$\frac{d}{dt} H_{\text{reflux\_tank}} = V_0 - L_0 - D$$

$$H_{\text{reflux\_tank}} \frac{d}{dt} x_{\text{reflux\_tank}} = V_0(x_{\text{in}} - x_{\text{reflux\_tank}}) \quad (A.26)$$

Liquid Flow Rates. The equations for the liquid flow rates are

$$L_{i,j} = L_0 R_L \qquad i = 1, ..., 8 \quad (A.27)$$

$$L_{i,j} = L_0 R_L + qF_0 \qquad i = 9, ..., 16 \quad (A.28)$$

$$L_{i,j} = L_0 \qquad i = 17, ..., 24 \quad (A.29)$$

$$L_{i,j} = L_0(1 - R_L) \qquad i = 25, ..., 32 \quad (A.30)$$

$$L_{i,j} = L_0(1 - R_L) - S \qquad i = 33, ..., 40 \quad (A.31)$$

$$L_{i,j} = L_0 + qF_0 - S \qquad i = 41, ..., 48 \quad (A.32)$$

Vapor Flow Rates. The equations for the vapor flow rates are

$$V_{i,j} = V_0 R_V + (1 - q)F_0 \qquad i = 1, ..., 8 \quad (A.33)$$

$$V_{i,j} = V_0 R_V \qquad i = 9, ..., 16 \quad (A.34)$$

$$V_{i,j} = V_0 R_V + (1 - q)F_0 + V_0(1 - R_V) \qquad i = 17, ..., 24 \quad (A.35)$$

$$V_{i,j} = V_0(1 - R_V) \qquad i = 25, ..., 32 \quad (A.36)$$

$$V_{i,j} = V_0(1 - R_V) \qquad i = 33, ..., 40 \quad (A.37)$$

$$V_{i,j} = V_0 \qquad i = 41, ..., 48 \quad (A.38)$$

Note that the DWC model considered in this work makes use of theoretical stages; hence there is no difference made in terms of column internals (trays or packing). Nevertheless, from a practical viewpoint, the HETP is assumed to be the same on both sides of the column if packing is used as internals. The potential HETP differences between the two sides of the column can be avoided by proper design as well as control measures.[2,9,48]

Notation

B = bottom product flow rate
D = distillate product flow rate
$\mathbf{d}$ = disturbance vector
e = error signal
F = feed flow rate
f, g = functions
f_{gain} = filter gain
F_L = closed loop transfer function
G_d = plant from the uncertainty set
G_s = shaped plant
H_i = liquid holdup
H_R = liquid holdup in reboiler
H_T = liquid holdup in reflux tank
$\mathbf{I}$ = identity matrix
K = controller
K_1, K_2 = control constants
k_i = constant hydraulic factor $i \in \{0, 1, 2\}$
K_r = reference tracking part of controller

K_y = output feedback part of controller
L_0 = reflux flow rate
n = noise signal
N = number of trays
P = plant
q = feed condition
$\mathbf{Q}$ = weight matrix on state
r = reference signal
$\mathbf{R}$ = weight matrix on input
R_L = ratio liquid split
R_V = ratio vapor split
S = side product flow rate
T = temperature
t = time
$\mathbf{u}$ = control vector
V_0 = vapor flow rate
$\mathbf{W}_1$ = precompensator matrix
$\mathbf{W}_2$ = postcompensator matrix
$\mathbf{W}_n$ = noise shaping filter
$\mathbf{W}_p$ = performance action weighting
$\mathbf{W}_u$ = control action weighting
$\mathbf{x}$ = state vector
x_A = top composition, component A
x_B = side composition, component B
x_C = bottom composition, component C
$x_{i,j}$ = liquid composition
$\mathbf{y}$ = output vector
$\mathbf{y}^*$ = set point vector
$y_{i,j}$ = vapor composition
z_1 = feed composition, component A
z_2 = feed composition, component B
α_j = relative volatility
$\mathbf{\Delta}$ = uncertainty matrix
Θ = time delay constant
μ_Δ = structured singular value

Subscripts

i = tray number $i \in \{1, ..., N\}$
j = component $j \in \{1, 2, 3\}$

Literature Cited

(1) Taylor, R.; Krishna, R.; Kooijman, H. Real-world modeling of distillation. *Chem. Eng. Prog.* **2003**, *99*, 28.

(2) Olujic, Z.; Kaibel, B.; Jansen, H.; Rietfort, T.; Zich, E.; Frey, G. Distillation column internals/configurations for process intensification. *Chem. Biochem. Eng. Q.* **2003**, *17*, 301.

(3) Petlyuk, F. B.; Platonov, V. M.; Slavinskii, D. M. Thermodynamically optimal method for separating multicomponent mixtures. *Int. Chem. Eng.* **1965**, *5*, 555.

(4) Kaibel, G. Distillation columns with vertical partitions. *Chem. Eng. Technol.* **1987**, *10*, 92.

(5) Christiansen, A. C.; Skogestad, S.; Liena, L. Complex distillation arrangements: Extending the Petlyuk ideas. *Comput. Chem. Eng.* **1997**, *21*, 237.

(6) Schultz, M. A.; Stewart, D. G.; Harris, J. M.; Rosenblum, S. P.; Shakur, M. S.; O'Brien, D. E. Reduce costs with dividing-wall columns. *Chem. Eng. Prog.* **2002**, (May), 64.

(7) Kolbe, B.; Wenzel, S. Novel distillation concepts using one-shell columns. *Chem. Eng. Process.* **2004**, *43*, 339.

(8) Becker, H.; Godorr, S.; Kreis, H. Partitioned distillation columns—why, when & how. *J. Chem. Eng.* **2001**, (Jan), 68.

(9) Kaibel, B.; Jansen, H.; Zich, E.; Olujic, Z. Unfixed dividing wall technology for packed and tray distillation columns. *Distill. Absorpt.* **2006**, *152*, 252.

(10) Isopescu, R.; Woinaroschy, A.; Draghiciu, L. Energy reduction in a divided wall distillation column. *Rev. Chim.* **2008**, *59*, 812.

(11) Kiss, A. A.; Pragt, H.; van Strien, C. Reactive Dividing-Wall Columns—How to get more with less resources. *Chem. Eng. Commun.* **2009**, *196*, 1366.

(12) Perry, R. H.; Green, D. W. *Perry's chemical engineers' handbook*, 8th ed.;McGraw-Hill: New York, 2008.

(13) Mueller, I.; Kenig, E. Y. Reactive distillation in a Dividing Wall Column—rate-based modeling and simulation. *Ind. Eng. Chem. Res.* **2007**, *46*, 3709.

(14) Wang, S. J.; Wong, D. S. H. Controllability and energy efficiency of a high-purity divided wall column. *Chem. Eng. Sci.* **2007**, *62*, 1010.

(15) Viel, F.; Busvelle, A.; Gauthiers, J. P. A stable control structure for binary distillation columns. *Int. J. Control* **1997**, *67*, 475.

(16) Rouchon, P. Dynamic simulation and nonlinear control of distillation columns. Ph.D. Thesis, Ecole des Mines de Paris, France, 1990.

(17) Isidori, A. *Nonlinear control systems: an introduction*; Springer-Verlag: New York, 1989.

(18) Biswas, P. P.; Ray, S.; Samanta, A. N. Multi-objective constraint optimizing IOL control of distillation column with nonlinear observer. *J. Process Control* **2007**, *17*, 73.

(19) Lee, P. L.; Sullivan, G. R. Generic Model Control (GMC). *Comput. Chem. Eng.* **1988**, *12*, 573.

(20) Rani, K. Y.; Gangiag, K. Adaptive Generic Model Control: dual composition control of distillation. *AIChE J.* **1991**, *37*, 1634.

(21) To, L. C. Nonlinear control techniques in alumina refineries. Ph.D. Thesis, Curtin University of Technology, 1996.

(22) Gu, D. W.; *Robust control design with Matlab*; Springer: New York, 2005; Chapter 11.

(23) Halvorsen, I. J.; Skogestad, S. Optimizing control of Petlyuk distillation: understanding the steady-state behaviour. *Comput. Chem. Eng.* **1997**, *21*, 249.

(24) Serra, M.; Espuña, A.; Puigjaner, L. Control and optimization of the divided wall column. *Chem. Eng. Process.* **1999**, *38*, 549.

(25) Serra, M.; Espuña, A.; Puigjaner, L. Study of the divided wall column controllability: influence of design and operation. *Comput. Chem. Eng.* **2000**, *24*, 901.

(26) Kiss, A. A.; Bildea, C. S.; Dimian, A. C.; Iedema, P. D. State multiplicity in CSTR-Separator-Recycle polymerization systems. *Chem. Eng. Sci.* **2002**, *57*, 535.

(27) Kiss, A. A.; Bildea, C. S.; Dimian, A. C.; Iedema, P. D. State multiplicity in PFR-Separator-Recycle polymerization systems. *Chem. Eng. Sci.* **2003**, *58*, 2973.

(28) Kiss, A. A.; Bildea, C. S.; Dimian, A. C. Design and control of recycle systems by non-linear analysis. *Comput. Chem. Eng.* **2007**, *31*, 601.

(29) Adrian, R.; Schoenmakers, H.; Boll, M. MPC of integrated unit operations: Control of a DWC. *Chem. Eng. Process.* **2004**, *43*, 347.

(30) Alstad, V.; Skogestad, S. Null space method for selecting optimal measurement combinations as controlled variables. *Ind. Eng. Chem. Res.* **2007**, *46*, 846.

(31) Suphanit, B.; Bischert, A.; Narataruksa, P. Exergy loss analysis of heat transfer across the wall of the dividing-wall distillation column. *Energy* **2007**, *32*, 2121.

(32) Il Kim, K.; Lee, M.; Park, S. Dynamic simulation for the structural design of the divided wall column for different feed composition and various separation features. In *International Conference on Control, Automation and Systems*; Seoul, Korea, October 17−20, 2007; pp 235−239.

(33) Ling, H.; Luyben, W. L. New control structure for divided-wall columns. *Ind. Eng. Chem. Res.* **2009**, *48*, 6034.

(34) Cho, Y.; Kim, B.; Kim, D.; Han, M.; Lee, M. Operation of divided wall column with vapor sidedraw using profile position control. *J. Process Control* **2009**, *19*, 932.

(35) Ordys, A.; Uduehi, D.; Johnson, M. *Process control performance assessment—from theory to implementation*; Springer: London, 2007.

(36) Skogestad, S. Dynamics and control of distillation columns—a critical survey. *IFAC-symposium DYCORD+'92*, Maryland, 1992, April 27−29.

(37) *MATLAB—Robust Control Toolbox Manual*; MathWorks Inc., 2007.

(38) Johnson, M. A.; Moradi, H. *PID control: new identification and design methods*; Springer-Verlag: London, 2005.

(39) Skogestad, S.; Postlethwaite, I. *Multivariable Feedback Control*, 2nd ed.; Wiley: New York, 2005.

(40) Signal, P. D.; Lee, P. L. Robust stability and performance analysis of Generic Model Control. *Chem. Eng. Commun.* **1993**, *124*, 55.

(41) Srinivasan, R.; Rengaswamy, R. Control loop performance assessment. 1. A qualitative approach for stiction diagnosis. *Ind. Eng. Chem. Res.* **2005**, *44*, 6708.

(42) Shoukat Choudhury, M. A. A.; Shah, S. L.; Thornhill, N. F.; Shook, D. S. Automatic detection and quantification of stiction in control valves. *Control Eng. Pract.* **2006**, *14*, 1395.

(43) Kiss, A. A.; Agachi, S. P. Model Predictive Control of temperature of a PVC emulsion process. *Hung. J. Ind. Chem.* **1999**, *27*, 117.

(44) Nagy, Z. K.; Mahn, B.; Franke, R.; Allgöwer, F. Evaluation study of an efficient output feedback nonlinear model predictive control for temperature tracking in an industrial batch reactor. *Control Eng. Pract.* **2007**, *15*, 839.

(45) Simon, L. L.; Kencse, H.; Hungerbuhler, K. Optimal rectification column, reboiler vessel, connection pipe selection and optimal control of batch distillation considering hydraulic limitations. *Chem. Eng. Process.* **2008**, *48*, 938.

(46) Simon, L. L.; Nagy, Z. K.; Hungerbuhler, K. Model based control of a liquid swelling constrained batch reactor subject to recipe uncertainties. *Chem. Eng. J.* **2009**, *153*, 151.

(47) Roman, R.; Nagy, Z. K.; Cristea, M. V.; Agachi, S. P. Dynamic modelling and nonlinear model predictive control of a Fluid Catalytic Cracking Unit. *Comput. Chem. Eng.* **2009**, *33*, 605.

(48) Kister, H. Can we believe the simulation results? *Chem. Eng. Prog.* **2002**, (Oct), 52.

Received for review July 2, 2009
Revised manuscript received October 19, 2009
Accepted October 20, 2009

IE9010673